2008-12

Investigation of new materials and methods of construction of personnel armor

Poh, Choon Wei.

Monterey California. Naval Postgraduate School

NAVAL POSTGRADUATE SCHOOL

MONTEREY, CALIFORNIA

THESIS

INVESTIGATION OF NEW MATERIALS AND METHODS OF CONSTRUCTION OF PERSONNEL ARMOR

by

Poh, Choon Wei

December 2008

Thesis Advisor:	Robert S. Hixson
Second Reader:	Jose O. Sinibaldi

Approved for public release; distribution is unlimited.

THIS PAGE INTENTIONALLY LEFT BLANK

REPORT DOCUMENTATION PAGE		Form Approved OMB No. 0704-0188

1. AGENCY USE ONLY *(Leave blank)*	2. REPORT DATE December 2008	3. REPORT TYPE AND DATES COVERED Master's Thesis

4. TITLE AND SUBTITLE Investigation of New Materials and Methods of Construction of Personnel Armor	5. FUNDING NUMBERS
6. AUTHOR(S) Poh, Choon Wei	
7. PERFORMING ORGANIZATION NAME(S) AND ADDRESS(ES) Naval Postgraduate School Monterey, CA 93943-5000	8. PERFORMING ORGANIZATION REPORT NUMBER
9. SPONSORING /MONITORING AGENCY NAME(S) AND ADDRESS(ES) N/A	10. SPONSORING/MONITORING AGENCY REPORT NUMBER

11. SUPPLEMENTARY NOTES The views expressed in this thesis are those of the author and do not reflect the official policy or position of the Department of Defense or the U.S. Government.

12a. DISTRIBUTION / AVAILABILITY STATEMENT Approved for public release; distribution is unlimited.	12b. DISTRIBUTION CODE A

13. ABSTRACT (maximum 200 words)

There has been a considerable amount of research done over the years on personnel and vehicle armor. However, much of this work has focused on finding materials that were very 'strong' to resist penetration of objects moving at high velocity. It is proposed here to study new armor concepts that are constructed using fundamental shock physics methods. The goal of this research is to develop materials concepts through an understanding of shock physics that will lead to new armor concepts for personnel, or for vehicles.

It is envisioned that initial concepts will be developed from theoretical arguments, but with the aid of computational tools, such as hydrocodes. Our approach is to define materials theoretically that have desirable properties, and put these materials together into a computer model.

It is also envisioned that at a minimum a four-layered approach is required. Currently, our concept is composed of an initial high impedance layer, which will serve to minimize the shock transmitted from an incoming blast wave. Additional layers are then optimized to stop projectile penetration. The second layer is envisioned to be able to quickly spread the energy from impact laterally coupled with a slow through-thickness sound speed for slowing down the shock wave. The third layer is then used to absorb energy much more effectively and transform kinetic energy into heat. If a fragment is still able to penetrate through layers 1, 2 and 3, it is essential to have a fourth layer with very high strength to provide a final attempt at stopping any penetrator.

14. SUBJECT TERMS High impedance, wave-spreading, porous, personnel armor	15. NUMBER OF PAGES 95
	16. PRICE CODE

17. SECURITY CLASSIFICATION OF REPORT	18. SECURITY CLASSIFICATION OF THIS PAGE	19. SECURITY CLASSIFICATION OF ABSTRACT	20. LIMITATION OF ABSTRACT
Unclassified	Unclassified	Unclassified	UU

NSN 7540-01-280-5500

Standard Form 298 (Rev. 8-98)
Prescribed by ANSI Std. Z39.18

THIS PAGE INTENTIONALLY LEFT BLANK

Approved for public release; distribution is unlimited.

INVESTIGATION OF NEW MATERIALS AND METHODS OF CONSTRUCTION OF PERSONNEL ARMOR

Poh, Choon Wei
Captain, The Singapore Army
B.E., The University of New South Wales, 2004

Submitted in partial fulfillment of the
requirements for the degree of

MASTER OF SCIENCE IN COMBAT SYSTEMS SCIENCES AND TECHNOLOGY

from the

NAVAL POSTGRADUATE SCHOOL
December 2008

Author: Poh, Choon Wei

Approved by: Dr. Robert S. Hixson
Thesis Advisor

Dr. Jose O. Sinibaldi
Second Reader

Dr. James H. Luscombe
Chairman, Department of Physics

THIS PAGE INTENTIONALLY LEFT BLANK

ABSTRACT

There has been a considerable amount of research done over the years on personnel and vehicle armor. However, much of this work has focused on finding materials that were very 'strong' to resist penetration of objects moving at high velocity. It is proposed here to study new armor concepts that are constructed using fundamental shock physics methods. The goal of this research is to develop materials concepts through the understanding of shock physics that will lead to new armor concepts for personnel.

It is envisioned that initial concepts will be developed from theoretical arguments, but with the aid of computational tools, such as hydrocodes. Our approach is to define materials theoretically that have desirable properties, and put these materials together into a computer model.

It is also envisioned that at a minimum a four-layered approach is required. Currently, our concept is composed of an initial high impedance layer, which will serve to minimize the shock transmitted from an incoming blast wave. Additional layers are then optimized to stop projectile penetration. The second layer is envisioned to be able to quickly spread the energy from impact laterally coupled with a slow through-thickness sound speed for slowing down the shock wave. The third layer is then used to absorb energy much more effectively and transform kinetic energy into heat. If a fragment is still able to penetrate through layers 1, 2 and 3, it is essential to have a fourth layer with very high strength to provide a final attempt at stopping any penetrator.

Results of this approach to a particular impact problem are presented. It is clear from our results that these ideas have merit.

THIS PAGE INTENTIONALLY LEFT BLANK

TABLE OF CONTENTS

I. INTRODUCTION 1
A. MOTIVATION 1
B. RESEARCH GOAL 2
C. RESEARCH OBJECTIVES 3
1. Outer Layer 4
2. Wave-Spreading Layer 4
3. Crush Layer 5
4. Final Stopping/Comfort Layer 6

II. BACKGROUND 9
A. SMALL ARMS AMMUNITION 9
B. CHARACTERISTICS OF 5.56 MM CARTRIDGES 10
C. CHARACTERISTICS OF 7.62 MM CARTRIDGES 11

III. SIMULATION TECHNICAL APPROACH 13
A. AUTODYN™ HYDROCODE 13
B. GENERAL HYDROCODE SETTINGS 13
1. 2 Dimensional (2D) Axial Symmetric 13
2. Lagrange Solver 13
3. Zoning 14
4. Gauges 14
5. Erosion 14
C. CODE VALIDATION 15
1. Simulation Setup 15
2. Simulation Results and Analysis 16

IV. OUTER LAYER SIMULATION STUDIES 19
A. INTRODUCTION 19
B. SIMULATION SETUP 20
C. SIMULATION RESULTS AND ANALYSIS 21

V. WAVE-SPREADING LAYER SIMULATION STUDIES 27
A. INTRODUCTION 27
B. SIMULATION SETUP 28
C. SIMULATION RESULTS AND ANALYSIS 32
1. High Sound Speed Target Plate Results and Analysis 32
2. Low Sound Speed Target Plate Results and Analysis 36
3. Layered Target Plate Results and Analysis 40
4. Comparison of Results 43

VI. CRUSH LAYER SIMULATION STUDIES 45
A. INTRODUCTION 45
B. SIMULATION SETUP 46
C. SIMULATION RESULTS AND ANALYSIS 48

VII. FINAL STOPPING LAYER SIMULATION STUDIES 53
A. INTRODUCTION 53
B. SIMULATION SETUP 53
C. SIMULATION RESULTS AND ANALYSIS 55
VIII. LAYERED TARGET PLATE SIMULATION STUDIES 59
A. INTRODUCTION 59
B. SIMULATION SETUP 59
C. SIMULATION RESULTS AND ANALYSIS 62
1. Steel Target Plate Results and Analysis 62
2. Layered Target Plate Results and Analysis 65
3. Comparison of Penetration Effects 68
IX. CONCLUSIONS AND RECOMMENDATIONS 73
A. CONCLUSIONS 73
B. RECOMMENDATIONS FOR FUTURE WORKS 73
1. Exploring Existing Materials 73
2. Simulation Setup 74
3. Experimental Testing 74
APPENDIX A. NOTATION 75
A. GLOSSARY OF TERMS AND NOTATION 75
LIST OF REFERENCES 77
INITIAL DISTRIBUTION LIST 79

LIST OF FIGURES

Figure 1. Example of Armor Concept. 6
Figure 2. Components of a Cartridge. 9
Figure 3. Components of a Full Metal Jacket Cartridge. 10
Figure 4. Plate Impact Simulation Setup. 16
Figure 5. Pressure versus Time Plot of Plate Impact Simulation. 17
Figure 6. Pressure Plot of Plate Impact Simulation. 18
Figure 7. Outer Layer Simulation Setup. 20
Figure 8. Zoom in of Outer Simulation Setup. 21
Figure 9. Pressure versus Time Plot of the Outer Layer. 22
Figure 10. Pressure Plot of Gauge 1 at Initial Impact of Outer Layer. 23
Figure 11. Impact Pressure at Gauge 1 of Outer Layer. 23
Figure 12. Pressure Plot of Gauge 7 at Initial Impact of Outer Layer. 24
Figure 13. Impact Pressure at Gauge 7 of Outer Layer. 25
Figure 14. Lagrange 2D Axial Symmetry Setup. 29
Figure 15. Layered Target Plate Simulation Setup. 30
Figure 16. Zoom In of Entire Simulation Setup. 31
Figure 17. Pressure versus Time Plot of the High Sound Speed Target Plate. 33
Figure 18. Pressure Plot of Gauge 1 at Initial Impact of High Sound Speed Target. 34
Figure 19. Impact Pressure at Gauge 1 of High Sound Speed Target. 34
Figure 20. Pressure Plot of Gauge 7 at Rear Surface of High Sound Speed Target. 35
Figure 21. Rear Surface Pressure at Gauge 7 of High Sound Speed Target. 36
Figure 22. Pressure versus Time Plot of the Low Sound Speed Target Plate. 37
Figure 23. Pressure Plot of Gauge 1 at Initial Impact of Low Sound Speed Target. 38
Figure 24. Impact Pressure at Gauge 1 of Low Sound Speed Target. 38
Figure 25. Pressure Plot of Gauge 7 at Rear Surface of Low Sound Speed Target. 39
Figure 26. Rear Surface Pressure at Gauge 7 of Low Sound Speed Target. 39
Figure 27. Pressure versus Time Plot of the Layered Target Plate. 40
Figure 28. Pressure Plot of Gauge 1 at Initial Impact of Layered Target. 41
Figure 29. Impact Pressure at Gauge 1 of Layered Target. 42
Figure 30. Pressure Plot of Gauge 7 at Rear Surface of Layered Target. 42
Figure 31. Rear Surface Pressure at Gauge 7 of Layered Target. 43
Figure 32. Comparison of Residual Energy between Solid and Porous Material. 45
Figure 33. Crush Layer Simulation Setup. 46
Figure 34. Zoom in of Crush Layer Simulation Setup. 47
Figure 35. Pressure versus Time Plot of the Crush Layer. 49
Figure 36. Pressure Plot of Gauge 1 at Initial Impact of Crush Layer. 49
Figure 37. Impact Pressure at Gauge 1 of Crush Layer. 50

Figure 38. Pressure Plot of Gauge 6 at Rear Surface of Crush Layer. 51
Figure 39. Impact Pressure at Gauge 6 of Crush Layer. 51
Figure 40. Final Layer Simulation Setup. 53
Figure 41. Zoom in of Final Layer Simulation Setup. 54
Figure 42. Pressure versus Time Plot of the Final Layer. 56
Figure 43. Pressure Plot of Gauge 1 at Initial Impact of Final Layer. 56
Figure 44. Impact Pressure at Gauge 1 of Final Layer. 57
Figure 45. Pressure Plot of Gauge 7 at Rear Surface of Final Layer. 57
Figure 46. Impact Pressure at Gauge 7 of Final Layer. 58
Figure 47. Steel Target Plate Simulation Setup. 60
Figure 48. Layered Target Plate Simulation Setup. 61
Figure 49. Zoom in of Layered Target Plate Simulation Setup. 62
Figure 50. Pressure versus Time Plot of the Steel Target Plate. 63
Figure 51. Pressure Plot of Gauge 1 at Initial Impact of Steel Target Plate. 63
Figure 52. Impact Pressure at Gauge 1 of Steel Target Plate. 64
Figure 53. Pressure Plot of Gauge 17 at Rear Surface of Steel Target Plate. 64
Figure 54. Impact Pressure at Gauge 17 of Steel Target Plate. 65
Figure 55. Pressure versus Time Plot of the Layered Target Plate. 66
Figure 56. Pressure Plot of Gauge 1 at Initial Impact of Layered Target Plate. 66
Figure 57. Impact Pressure at Gauge 1 of Layered Target Plate. 67
Figure 58. Pressure Plot of Gauge 17 at Rear Surface of Layered Target Plate. 67
Figure 59. Impact Pressure at Gauge 17 of Layered Target Plate. 68
Figure 60. Penetration Depth of Steel Target Plate. 69
Figure 61. Final Velocity of Projectile of Steel Target Plate. 69
Figure 62. Penetration Depth of Layered Target Plate. 70
Figure 63. Final Velocity of Projectile of Layered Target Plate. 71
Figure 64. Velocity of Projectile of Layered Target Plate at 45μs. 71

LIST OF TABLES

Table 1. Ballistic Data for 5.56 mm Cartridges. 11
Table 2. Ballistic Data for 7.62 mm Cartridges. 11
Table 3. Material Properties of Outer Layer Simulation. 21
Table 4. Properties of Innovative Materials. 28
Table 5. Material Properties of Wave-spreading Layer. 31
Table 6. Simulation Results for Impact and Rear Surface Pressure. 44
Table 7. Material Properties of Crush Layer Simulation. 48
Table 8. Material Properties of Final Layer Simulation. 55
Table 9. Material Properties of Steel Target Plate Simulation. 60
Table 10. Comparison between Steel and Layered Target Plate. 72

THIS PAGE INTENTIONALLY LEFT BLANK

ACKNOWLEDGMENTS

This thesis research would not be possible without the unwavering assistance and support from my thesis advisors. I would like to express my gratitude and appreciation to them.

Dr. Hixson for offering his vast wealth of experience in this field of research. He is always available and patience in providing advices to the many questions. He is invaluable in his guidance, support and firm leadership through the course of this research.

Dr. Sinibaldi for his extensive guidance and time in the simulation setups for AUTODYN™. His patience and time offered in going through the simulation setup has accelerated the process of this research.

THIS PAGE INTENTIONALLY LEFT BLANK

I. INTRODUCTION

A. MOTIVATION

This research supports current DoD effects to develop new ways to protect personnel and vehicles. Improvised explosives devices (IEDs) have become a common threat in many areas, including the current operational scenario and is been used extensively in Iraq against the coalition forces. To protect personnel and vehicles or other assets, it is important to have effective armor materials. Currently used vehicular armor, for example, is relatively heavy. Use of such armor is largely limited by the ability of the vehicle suspension system to carry the weight. Lighter armor (which could then be made thicker), or armor with similar weight but with better performance would allow for better protection and still good mobility.

An IED can cause damage in at least two ways. The first is cause by the blast wave that is caused by the high explosives product expansion driving a strong shock front into air. The second is the production of fragments or explosively formed projectiles (EFP) that can fly up to a velocity of 1.5 km/s and cause damage by impact. It is the second threat that is the principal focus of this research.

There has been a considerable amount of research done over the years on personnel and vehicle armor. However, much of this work has focused on finding materials that were very ‘strong’ to resist penetration of objects moving at high velocity. When a projectile hits a very strong material, the impactor absorbs much of the energy created by the impact event. But there is also considerable damage done to the target, because of the very localized nature of the impact. Even very strong materials still have elastic limits that are still very small compared to the stresses generated in very high velocity impacts. So it seems reasonable to look for ways to quickly reduce stress state in the target materials,

and to look for ways to convert kinetic energy to heat energy. In this way, we can minimize the chance that a fragment or projectile will penetrate the armor.

Therefore, the motivation here is to consider how the effect of a localized impact region can be spread out quickly, and how energy can be absorbed by new kinds of armor materials. Spreading out force over a very small area to that over a larger area during the transit time of the first shock wave will lead to lower stress at the back of the target materials, and thus reduce the possibility of penetration. If penetration can be stopped, the survivability of the target increases. It is proposed here to study new armor concepts that are constructed using fundamental shock physics methods, and to do direct comparison with a baseline material. We have chosen steel as the baseline material.

Naturally there are limits to the effectiveness of even advanced armor designs. We must recognize that we can provide protection for many threats, but it is difficult or impossible using current technology to protect against all threats. Very high velocity fragments or explosively formed projectiles are inherently difficult to protect against. So a part of this work was focused on summarizing the threats for small arms.

B. RESEARCH GOAL

The goal of this research is to develop materials concepts through the understanding of shock physics that will lead to new armor concepts for personnel. It is envisioned that initial concepts will be developed from theoretical arguments, but with the aid of computational tools, such as hydrocodes. Our approach is to define materials theoretically that have desirable properties, and put these materials together into a computer model. We then do computer simulations using a commercially available two-dimensional non-linear dynamic analysis program (AUTODYN^{tm}). We then will vary design and material properties to optimize the armor design. At a later stage, optimized concepts will be tested experimentally. The theoretical process described above gives us direction to guide experiments. Experiments are not a part of this research, but

are required in the future to be able to validate armor material designs. The results of future experiments will then be used to iterate on the design to better match experimental results. This gives us better confidence in the fidelity of future designs.

The focus will be on fragment and projectile penetration physics. It is clear that no one material can currently have all the properties necessary to mitigate fragments or projectiles, therefore this research will explore the possibility of using novel materials constructed in layers as a concept. Personal and vehicle protection have similarities, and our concepts can apply to either.

C. RESEARCH OBJECTIVES

While the research goal is to develop new armor concepts for personnel, in order to achieve this research goal, the concept of a layered approach sets the research objectives. Because no one material can have all the correct properties to mitigate against both blast effects and the localized impact form fragments or projectiles, we have defined an initial layered model in which each layer has specific desirable properties. Eventually, in future research we will look at defining composite materials where one layer will have more than one specific desirable property. At this point in our research, we will not worry about the difficulty of finding the materials required, but rather define theoretical materials to test the physical mechanisms. This will help determine the viability of the concept. Real material definition will take place in future research efforts. It is envisioned that at a minimum a four-layered approach is required. Currently, our concept is composed of an initial high impedance layer, which will serve to minimize the shock transmitted from an incoming blast wave. However it will not be optimized to stop a penetrating object. The second layer is envisioned to be able to quickly spread the energy from impact. The third layer is then used to absorb energy much more effectively and transform kinetic energy into heat. If a

fragment is still able to penetrate through layers 1, 2 and 3, it is essential to have a fourth layer with very high strength to provide a final attempt at stopping any penetrator.

1. Outer Layer

When a shock front in a low impedance material such as air reaches an interface with a much higher impedance material, a wave interaction occurs that causes the blast wave to be reflected; this depends upon the ratio of impedance of the materials in this layer to that of air. This ratio is so large for essentially any solid material that the blast wave will essentially double in amplitude upon reflection. By impedance we mean 'shock impedance' which is analogous to acoustic impedance: the product of the material density and the shock velocity. A shock is transmitted into the target and the amplitude of this shock is determined by the ratio of shock impedance in air to that in the metal layer. The nature of the shock driven into this layer by a triangular blast wave depends upon details of both air and the layer materials as well as the shape of the pressure pulse. We will not consider this problem in detail, but will focus on the problem of projectile or fragment penetration. For penetration resistance we wish to have relatively high mass and good ductility, so we have chosen tantalum as a representative material for this initial layer. This may not be a practical choice for real armor, but will allow us to test the physical concepts. It is relatively simple to define this kind of layer for vehicle protection, where it can be rigid. For personnel armor the situation is more difficult as a high shock impedance material that is also flexible will need to be found or designed.

2. Wave-Spreading Layer

When a fragment or projectile impacts a target, there will be an area of very localized loading on the target. The idea for this layer is to spread the force of the impact over the largest area possible to reduce the chances of localized penetration. This is called a 'wave-spreading' layer, and will probably eventually

require a specifically designed composite structure. This was looked at briefly by Gupta et al. [1, 2] but in a much different way than we describe here. For this study, we are creating a wave spreading material by using layers of more simple materials. The desirable property here is a very high lateral sound speed as compared to through thickness speed, which also implies a very high shock wave velocity. So if this layer is made of a material with a high sound speed, the through-thickness transit time will be fast, but the shock speed laterally will also be fast. This layer alone will not do all that we need the wave spreading layer to do. It must be combined with another layer with low wave velocities. This low sound speed layer will increase the overall transit time and allow more lateral wave spreading to occur. The use of layers here is just to test the physics and quantify the effectiveness of this approach. What is ultimately desired here is a single composite material that is very anisotropic. In other words, a single material that has very different wave propagation velocities in one direction compared to another direction. This kind of material is left to future research. One challenge for personnel protection armor, as for the above layer, is to find flexible materials for these layers.

3. Crush Layer

In this study, we use a porous material for this layer to absorb energy. Highly porous materials are well known to be able to absorb kinetic energy and turn it into heat energy. Typically, such materials are good only for a single use, as they can be irreversibly compacted when loaded to high stress. Fortunately porous polymeric materials are available that are known to be effective at absorbing kinetic energy and converting it into heat energy. In addition, polymeric foams can be found that are very flexible. For this study, we will actually use porous aluminum to test the physics concept because there are many existing models that can be used simply in the AUTODYN™ computer code.

4. Final Stopping/Comfort Layer

Finally, an inner stopping layer is envisioned for our layered design. For vehicular armor, this layer can be any appropriate penetration resistant material. For personnel armor, this layer can also serve to wick moisture away from the user and provide a final penetration layer. We envision this material to be very tough and penetration resistant, but also slightly porous to be able to 'wick' moisture away from the user. The final conceptual material for this research shown in Figure 1.

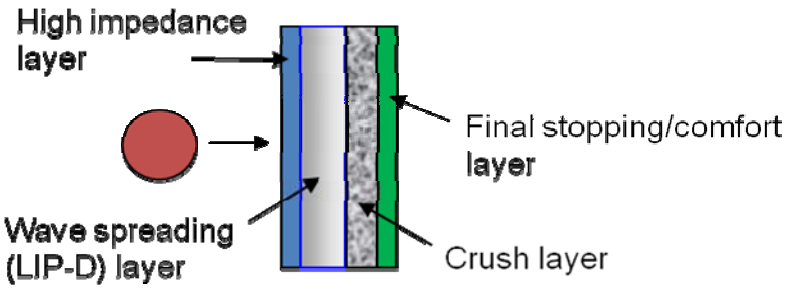

Figure 1. Example of Armor Concept.

This thesis consists of nine chapters documenting the approach and simulation results of the various layers and culminating with the results of the four-layered target plate followed by conclusions and recommendations. Chapter I and II introduce the motivation of this research and discuss on the background of possible threats against personnel armor respectively. Chapter III presents a short introduction on AUTODYN^{TM} and the general hydrocode settings used throughout the simulations for this research. It also covers a section on a simple pate impact simulation for code validation. Chapters IV to VII cover the simulation results and analysis of the various layers. Results were achieved through the various simulations and are discussed in these four chapters. Chapter VIII combines the results obtained from the previous chapters to test out the four-layered target plate approach. This is the first time that the various

layers are integrated together for simulation and results are compared with the baseline material of steel. Finally, the research conclusions are discussed in Chapter IX along with recommendations for future work.

THIS PAGE INTENTIONALLY LEFT BLANK

II. BACKGROUND

A. SMALL ARMS AMMUNITION

Personnel protection armor is designed to resist penetration from small arms ammunition (SAA) that is up to 7.62 millimeter in caliber. Small arms ammunition [3] also known as cartridges, are those used in rifles, handguns and machine guns and range in sizes from caliber .22 cartridges through to 30 millimeter cartridges. A cartridge consists of the projectile, casing, propellant, rim and primer all contained in one metal package as shown in Figure 2. The projectile has the capability of penetrating several millimeters into a steel plate and remains as one of the serious threats faced by individual solider in their daily deployment. It is important to understand the nature of the threat in order to be able to develop new forms of protection. Conversely, it is important to realize that all armor systems have limitations, including the system we are developing here.

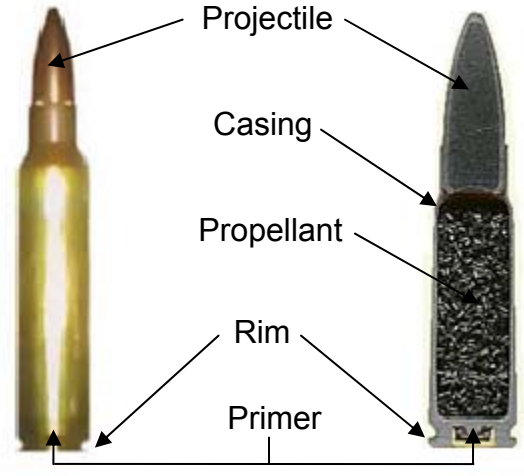

Figure 2. Components of a Cartridge.

B. CHARACTERISTICS OF 5.56 MM CARTRIDGES

Rifles such as the M16 and M249 use the 5.56 mm cartridges intended for use against personnel and light armored or armored targets. There are many types of 5.56mm cartridges designed for different usage, such as dummy cartridges for practice or testing of weapon mechanisms or tracer cartridges for visible observation of the projectile's trajectory to the point of impact.

Many development efforts over the years had looked into improving the penetration performance of this cartridge against personnel protection armor. The full metal jacket (FMJ) and the armor piercing (AP) projectile are design to have enhanced penetration capability against personnel protection armor due to the materials used in the projectile.

Figure 3 shows the cross section of a FMJ projectile consisting of a lead core encapsulate by a copper jacket. The jacket serves as a form of protection for the lead core when the projectile is passing through the barrel and during flight so as to allow the projectile to stay intact while impacting the target. This makes the FMJ projectile more effective at piercing armor and more durable. Similarly, the AP projectile has jacketed designs where the core material is made of very hard and/or high-density metal such as depleted uranium, hardened steel or tungsten.

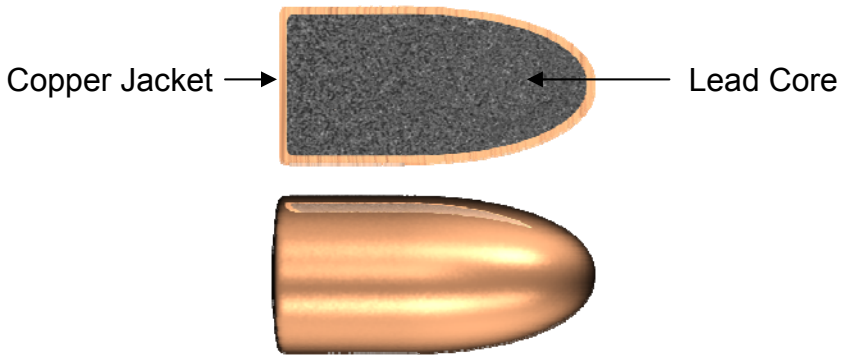

Figure 3. Components of a Full Metal Jacket Cartridge.

Table 1 summarizes the ballistic data of the 5.56 mm cartridges that have enhanced penetration performance.

Table 1. Ballistic Data for 5.56 mm Cartridges.

Model	Cartridge Weight	Cartridge Length	Projectile Weight	Projectile Length	Velocity
M193 Ball	11.79 g	57.4 mm	3.63 g	19.3 mm	975 m/s
M855 Ball	12.31 g	57.4 mm	4.02 g	23 mm	908 m/s
M995 AP	11.66 g	57.15 mm	3.37 g	-	997 m/s

C. CHARACTERISTICS OF 7.62 MM CARTRIDGES

The 7.62 mm cartridges offer similar ballistic performance to most ammunition. However, they are much more effective than the 5.56 mm cartridge at long range. These cartridges are commonly used in sniper rifles and general-purpose machine guns and the ballistic data are summarized in Table 2.

Table 2. Ballistic Data for 7.62 mm Cartridges.

Model	Cartridge Weight	Cartridge Length	Projectile Weight	Projectile Length	Velocity
M59 Ball	25.47 g	71.1 mm	9.75 g	32.5 mm	825 m/s
M61 AP	25.47 g	71.1 mm	9.75 g	32.5 mm	825 m/s
M80 Ball	25.4 g	71.1 mm	9.46 g	29 mm	825 m/s
M118 Special Ball	25.27 g	71.9 mm	11.15 g	33.3 mm	792 m/s
M993 AP	23.5 g	71.1 mm	8.2 g	-	896 m/s

THIS PAGE INTENTIONALLY LEFT BLANK

III. SIMULATION TECHNICAL APPROACH

A. AUTODYN™ HYDROCODE

The AUTODYN™ hydrocode [4, 5] was used for computer simulations throughout this research. AUTODYN™ is an engineering and scientific tool for solving complex non-linear dynamics problems such as shock and blast waves, explosions, impact and penetration, and solid, fluid and gas dynamics. It offers many finite-difference solvers such as Lagrange, Euler, Arbitrary Lagrange Euler and Smooth Particle Hydrodynamics. The Lagrange solver was used extensively in this research to study impact and penetration problems.

B. GENERAL HYDROCODE SETTINGS

There are several settings and manipulations available within AUTODYN™ for setting up a simulation. This discussion is not meant to be inclusive of all the possible combinations but will focus on the settings used in this research.

1. 2 Dimensional (2D) Axial Symmetric

The 2D axial symmetric simulation setup is the simplest form to model problems in which there is cylindrical symmetry. Models are symmetrical about a single axis thus giving it a cylindrical symmetry. This form of setup also causes the simulation to be computed in a shorter time. Axial symmetry has some issues with regard to overall conservation of energy, but these are not important for the work we describe here.

2. Lagrange Solver

The Lagrange solver is well suited for the description of solid materials. The Lagrange solver produces a mesh grid that overlays the material and moves with the material. In this case, the grid is continually deformed and refined during

the simulation. This is the natural coordinate system to use for shock wave interaction problems, and allows for simple calculations and fast run times. The Lagrange solver does have the ability to erode materials during the interaction with the ability to keep momentum on single point particles.

3. Zoning

Different zoning setups calculate and predict experimental results differently. Coarser zoning causes less accurate predicted experimental results. There is a natural trade off here. More zones per millimeter allows for higher fidelity simulations, but at the expense of very long computation time, and memory usage. Coarse zoning may cause some fine details to be lost. So we found a compromise zoning where we have good fidelity but with reasonable run times. The zoning for all simulations performed in this research is at four cells per millimeter in the region of interest.

4. Gauges

Gauges are predetermined fixed points within a particular computation space that measure and record the data that moves over the gauge. In the Lagrange solver, these fixed points remained fixed to the grid, however one must note that under large deformations, the grid does deform with the material deformation. The use of gauges allows particular points in the materials used to be closely examined for stress, strain, and other relevant dynamic properties. In this research, gauges were used to record the pressure of the shock waves propagating through the target plate. The output of these gauges were used to keep track of wave propagation and attenuation, principally in the target materials.

5. Erosion

Erosion is initiated for an element when the specified strain limit is reached. It is a setting used for Lagrange solvers that allows a node of particular

material to erode reducing the zoning of the material. This is necessary in some cases as severe deformation of material nodes can halt a simulation before completion.

C. CODE VALIDATION

A simple plate impact simulation was performed in order to validate the AUTODYN™ hydrocode. The simulation is a plate impact problem with plates made of the same materials. Because we can solve such a simple problem analytically, we have benchmark information that we can compare to the simulation results. Specifically, we can compare stress amplitudes, wave profiles, and propagation times from an analytical calculation with those from our simulation to be sure we have good agreement. This gives us confidence that we have set the simulations up correctly.

1. Simulation Setup

The plate impact simulation was performed using Lagrange solvers and it consists of a flyer plate (dark blue in color) that is 25 mm by 25 mm and a target plate (green in color) that is 25 mm by 5 mm as shown in Figure 4. To keep it simple, both plates are made of tantalum metal; this is called symmetric impact and has a particularly simple analytical solution. The flyer plate is moving at an initial velocity of 1000 m/s and gauges were set up within the target plate to measure the impact pressure as a function of propagation distance as a form of validation.

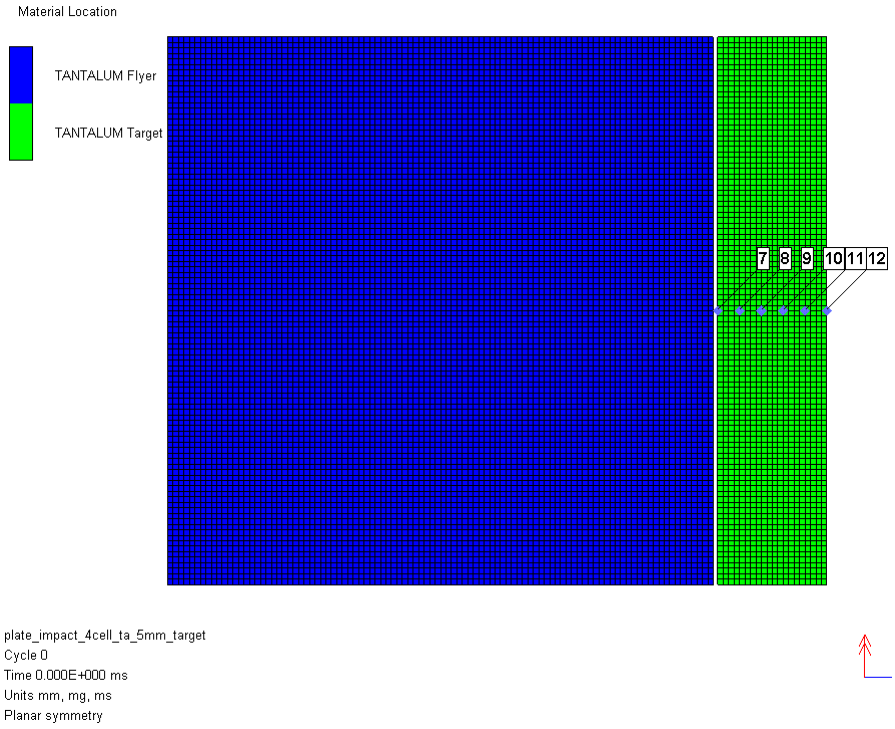

Figure 4. Plate Impact Simulation Setup.

2. Simulation Results and Analysis

The primary goal of this plate impact simulation was the validation of the AUTODYN™ hydrocode against analytically calculated results. The simulated impact pressure indicated in Figure 5 and 6 is about 33.43 GPa, while the calculated impact pressure is at 33.52 GPa. The analytical value is determined from the fact that particle velocity in the target is exactly half the flyer plate initial velocity, and from the shock wave jump conditions. There is good agreement between the two results. The small difference in results is probably due principally to the need for 'artificial viscosity' in the simulation to maintain stability. It is also clear from Figure 5 that the shock wave profiles at each gauge location are of the correct shape for a simple shock. That is, they show a fast rise, a flat top where there is uniform stress and a more gradual release when stress is decreased. The oscillations on the top of these wave profiles are caused by numerical instabilities. These can be damped out by increasing the artificial

viscosity [4, 5] but this will also affect the peak stress. So we must live with small oscillations. These results are both qualitatively and quantitatively correct, and give us confidence that we are setting up this simple problem correctly.

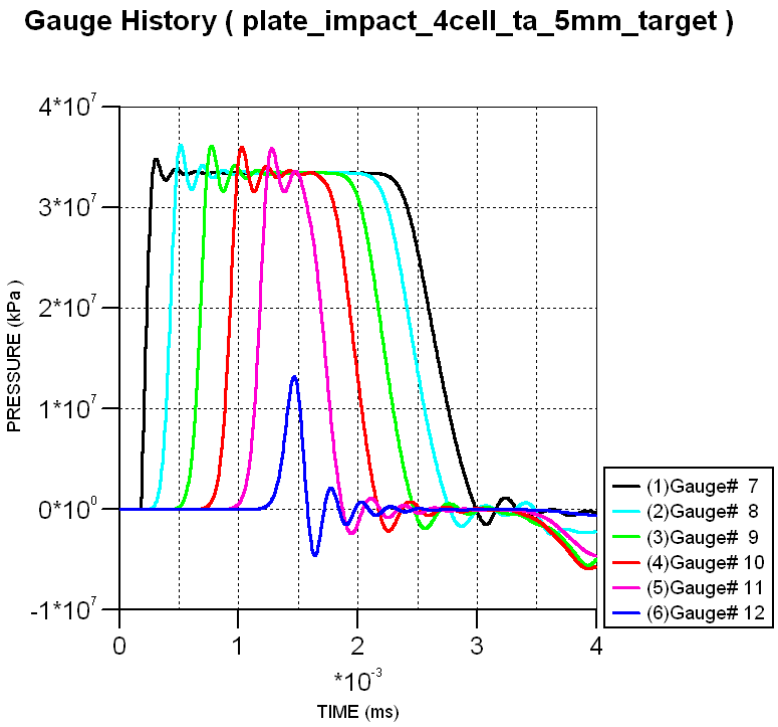

Figure 5. Pressure versus Time Plot of Plate Impact Simulation.

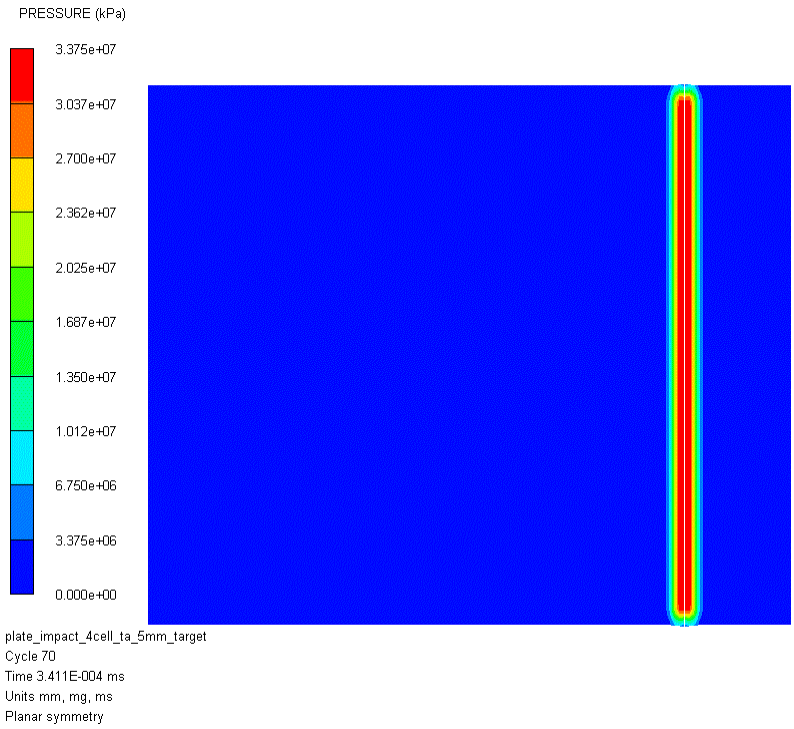

Figure 6. Pressure Plot of Plate Impact Simulation.

IV. OUTER LAYER SIMULATION STUDIES

A. INTRODUCTION

The approach for the personnel protection armor is to use fundamental principles of shock compression physics to investigate new armor concepts and materials. The idea is to make use of a layered approach to mitigate damage against blast effects and projectile impact. The use of layers is a first and very important step in this research, and will let us run relatively simple simulations to see if this concept has merit. If so, we can move on to more complex ideas using composite materials specifically designed to have desirable properties.

The idea for the first layer is to be able to reflect away as much blast wave energy as possible upon impact. Therefore, a layer of high density and ductile material is a good starting choice for this layer. When a shock wave in a low impedance material (such as air) reaches an interface with a much higher impedance material (such as a metal), a wave interaction occurs that causes pressure in the reflected wave to essentially double. We note here that we show no simulations of the blast wave in air interacting with our armor concept, but will focus our simulations on projectile or fragment impact.

In additional, the first layer should be a ductile material. Hard (brittle) materials will shatter relatively easily through the creation and propagation of cracks, but ductile materials will deform before failing. We have taken this outer layer to be thin, but of high initial density to maximize the mass. This will help with penetration resistance. We will make no attempt here to identify a suitable existing material, but will choose a high shock impedance material for our simulations. This also lets us test the problem setup and be sure we are obtaining physically meaningful results from this setup.

B. SIMULATION SETUP

The simulation is setup using the Lagrange solver in 2D axial symmetry with a tantalum projectile (dark blue in color) that has a length of 15 mm and a radius of 4 mm as shown in Figure 7, which only the top half of an axial symmetric body is shown. The target plate (green in color) has a thickness of 9 mm with 7 gauges set at 1.5 mm apart within the plate as shown in Figure 8. The velocity of the projectile is set at 1000 m/s and there is initially a gap of 0.2 mm between the projectile and the target plate.

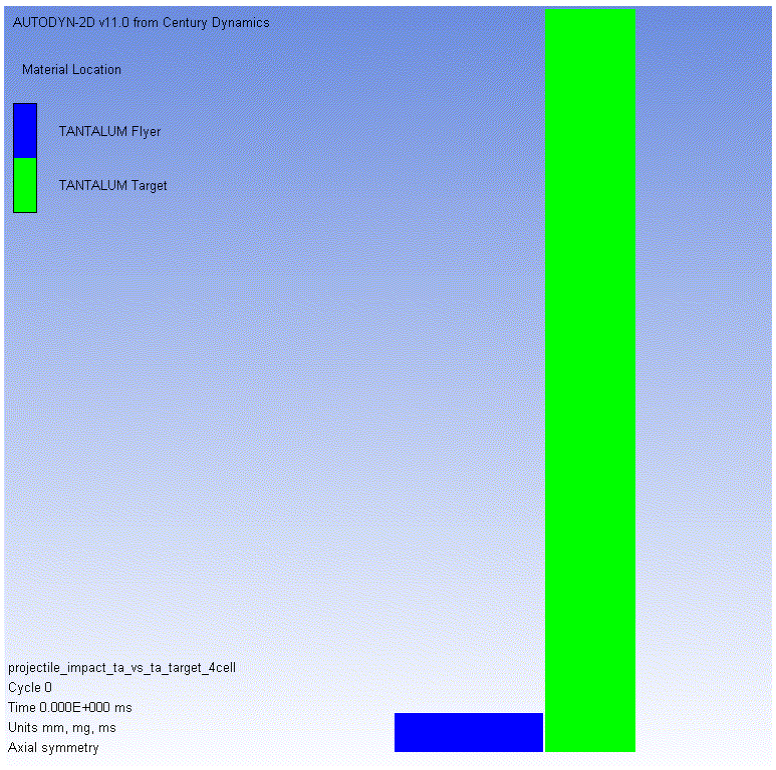

Figure 7. Outer Layer Simulation Setup.

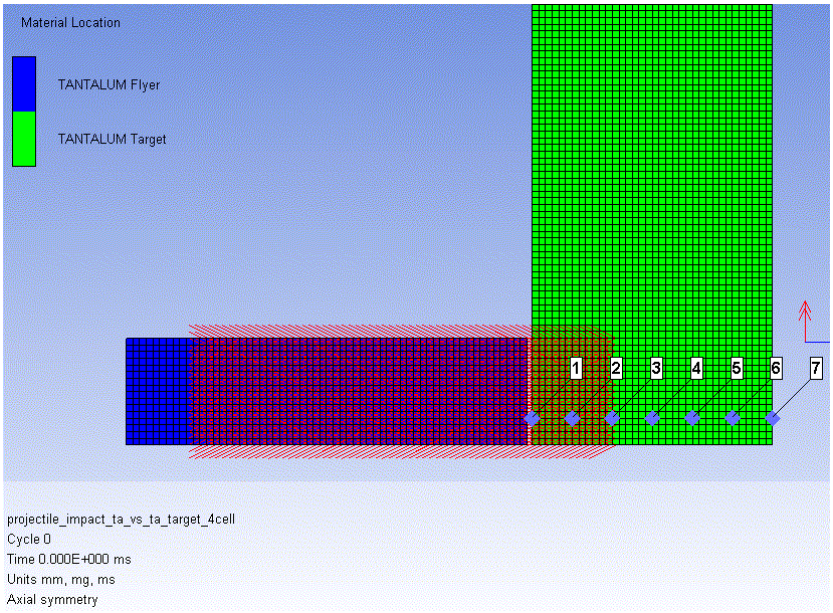

Figure 8. Zoom in of Outer Simulation Setup.

Table 3 summarizes the equation of state (EOS), strength model, failure model, and erosion criteria for the materials used in the simulation.

Table 3. Material Properties of Outer Layer Simulation.

Equation of State	**Strength Model**	**Failure Model**	**Erosion**
Tantalum			
Shock	Steinberg Guinan	Hydro (P_{min})	Geometric Strain
C = 3414 m/s S = 1.201	G = 69 GPa Y = 0.77 GPa	σ_{spall} = - 2 GPa	Strain = 2

C. SIMULATION RESULTS AND ANALYSIS

Figure 9 shows the pressure versus time plot of the shock wave propagating through the target plate at the various gauge locations. The shock wave takes about 2.47 μs to reach the last gauge at the rear surface of the plate

and it is clearly indicated in the plot that the pressure attenuates as the shock wave travels through the plate. We note that the wave profile for the first and second gauge locations have flat tops, where subsequent gauges profiles have a 'triangular' shape. The triangular wave shapes are caused by release waves originating from the edges of the impactor at the impact interface reaching the axis of the target and destroying the state of uniaxial strain that was there. These release waves are caused by the zero stress boundary condition that exists at free surfaces. This is an expected result and gives us further confidence in the computational model.

As shown in Figure 10 and 11, the initial impact pressure at the interface between the projectile and the target plate recorded by gauge 1 is about 33.9 GPa. This is in good agreement with the impact stress calculated analytically.

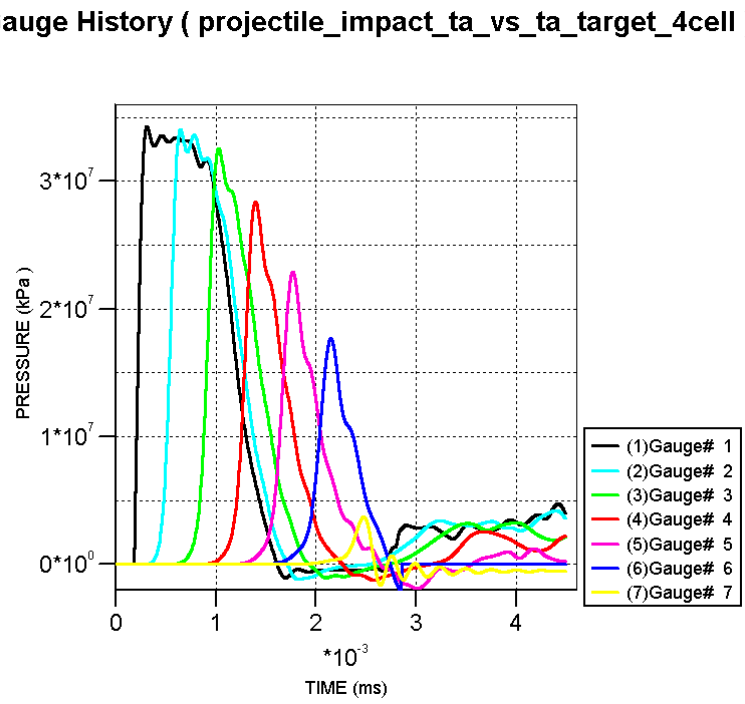

Figure 9. Pressure versus Time Plot of the Outer Layer.

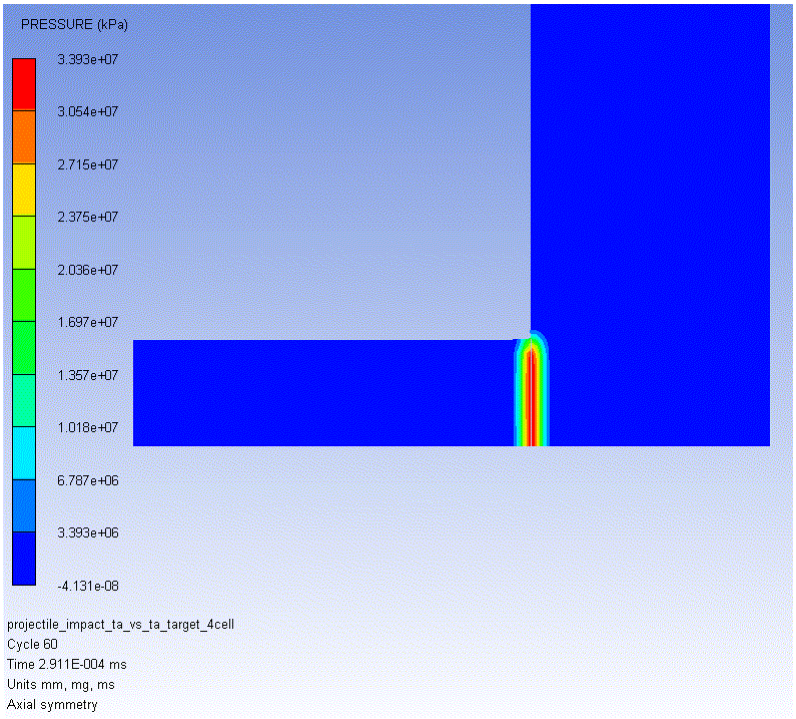

Figure 10. Pressure Plot of Gauge 1 at Initial Impact of Outer Layer.

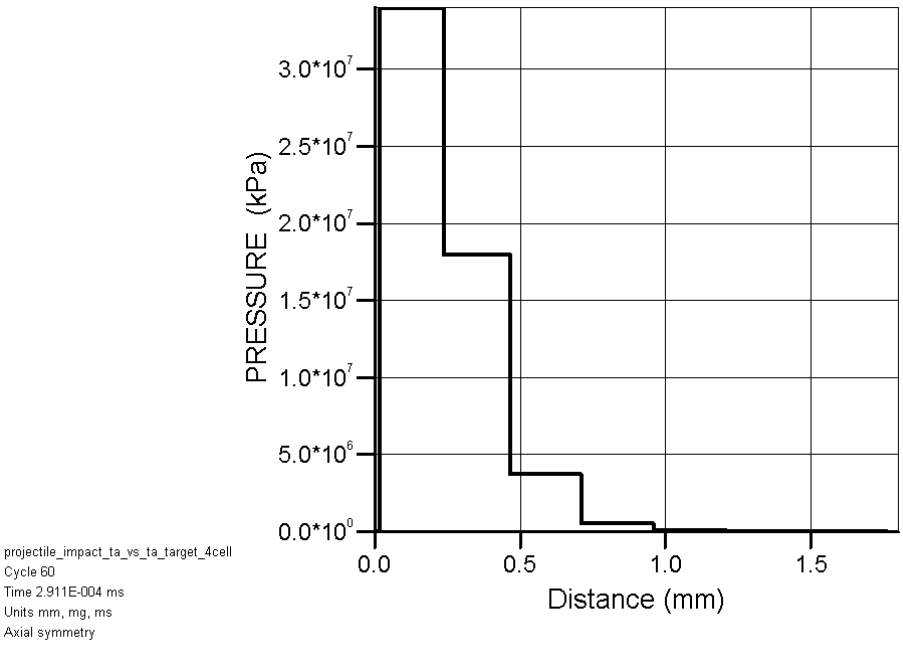

Figure 11. Impact Pressure at Gauge 1 of Outer Layer.

Figure 12 shows the pressure contour plot of the shock wave reaching the rear surface of the target plate. The last gauge located at the rear surface recorded a rear surface pressure of about 3.84 GPa as shown in Figure 13. That is a decrease in pressure of about 30 GPa from the initial impact pressure. Even though, there is a significant decrease in pressure at the rear surface there is still enough pressure to create concussion damage to personnel. Subsequent layers will serve to attenuate this stress wave further.

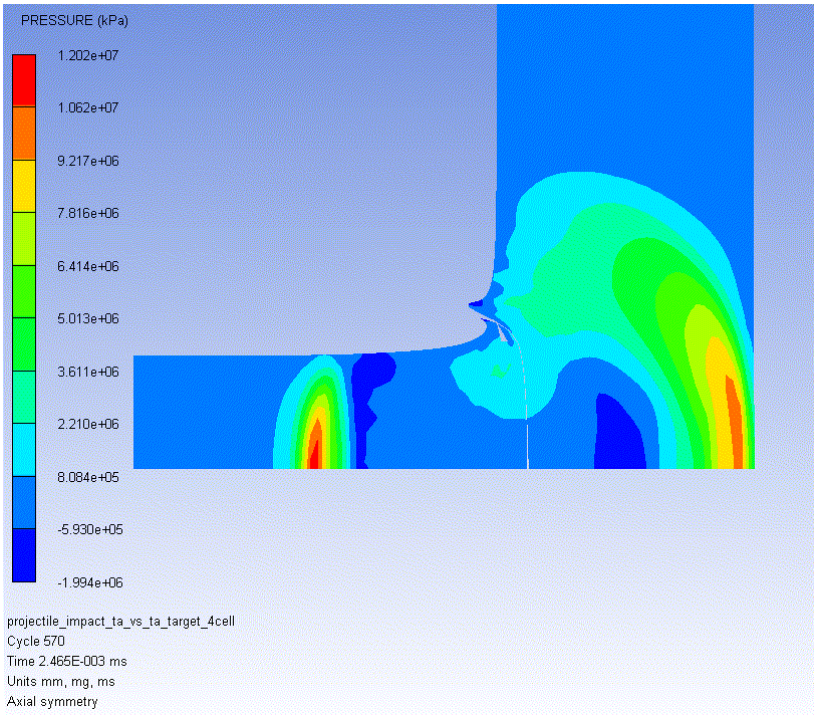

Figure 12. Pressure Plot of Gauge 7 at Initial Impact of Outer Layer.

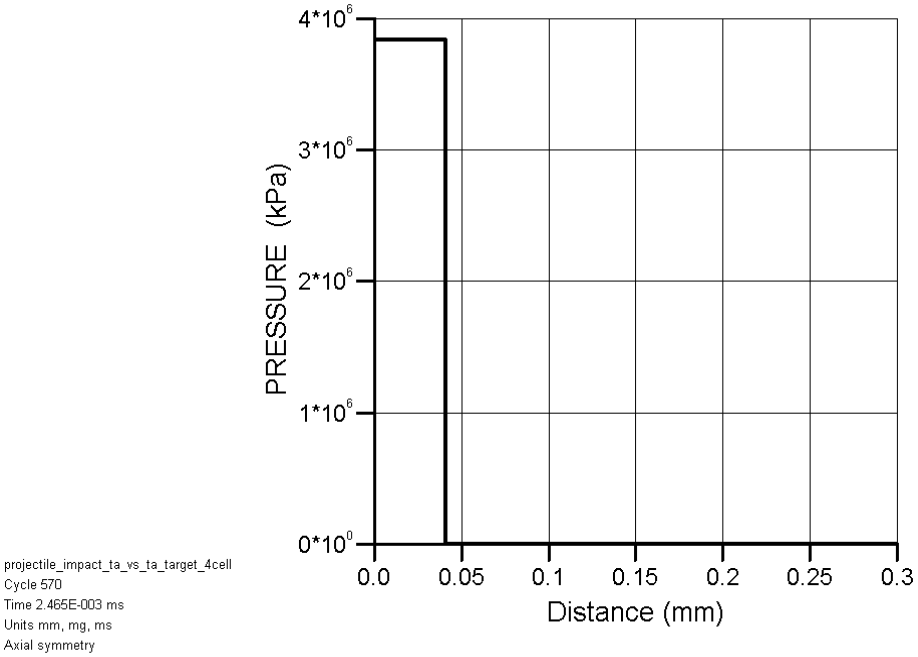

Figure 13. Impact Pressure at Gauge 7 of Outer Layer.

THIS PAGE INTENTIONALLY LEFT BLANK

V. WAVE-SPREADING LAYER SIMULATION STUDIES

A. INTRODUCTION

It is clear that no one material, excluding composite materials, can have all necessary properties to mitigate the penetration effects of a projectile travelling at high velocity. The idea for a wave-spreading layer [1, 2] is conceptually very simple; by spreading the force of a very small impact area out to a much larger area, the pressure state can be reduced. This, in turn will reduce the chances of penetration.

This leads us to look at innovative anisotropic materials that in addition to having parameters such as high strength and density to resist penetration, have a high lateral sound speed as compared to the through thickness sound speed so as to rapidly spread the locally applied impact and energy. This is coupled with a material that has a slow through-thickness sound speed for slowing down the shock wave to allow the lateral spreading to occur in the high wave speed material. This wave-spreading layer could also be a new composite material having the above properties.

For research purposes, innovative materials with desired properties of high and low sound speed have been defined in Table 4. These are theoretical choices, and so represent no real materials. Defining such materials this way allows us tailor properties to see if the fundamental concepts have value. Note that these materials have extreme differences in both bulk sound speed and in density, to test the effectiveness of the concept. These materials also follow 'Birch's law', which says that materials with low density have relatively high sound speed, and materials with high density have relatively low sound speeds.

Table 4. Properties of Innovative Materials.

Innovative Materials	Shock Velocity, U_s	Density, ρ_o	Impedance, Z
High Sound Speed	15 km/s + 1.5 u_p	3 g/cm^3	45
Low Sound Speed	1 km/s + 1.5 u_p	20 g/cm^3	20

B. SIMULATION SETUP

In order to understand the performance of the wave-spreading layer concept, three separate simulation setups were used to assess wave propagation caused by impact in the high sound speed, low sound speed and composite materials. These simulations were performed using Lagrange solvers in two dimensional (2D) axial symmetry.

In each setup, two Lagrange parts were created as shown in Figure 14. One part is the projectile (dark blue in color) and the other part is the target plate (green in color). The material for the projectile is tantalum and it is cylindrical with length of 15 mm and a radius of 4 mm. The material for the target plate is the innovative material of either high sound speed or low sound speed with a thickness of 9 mm.

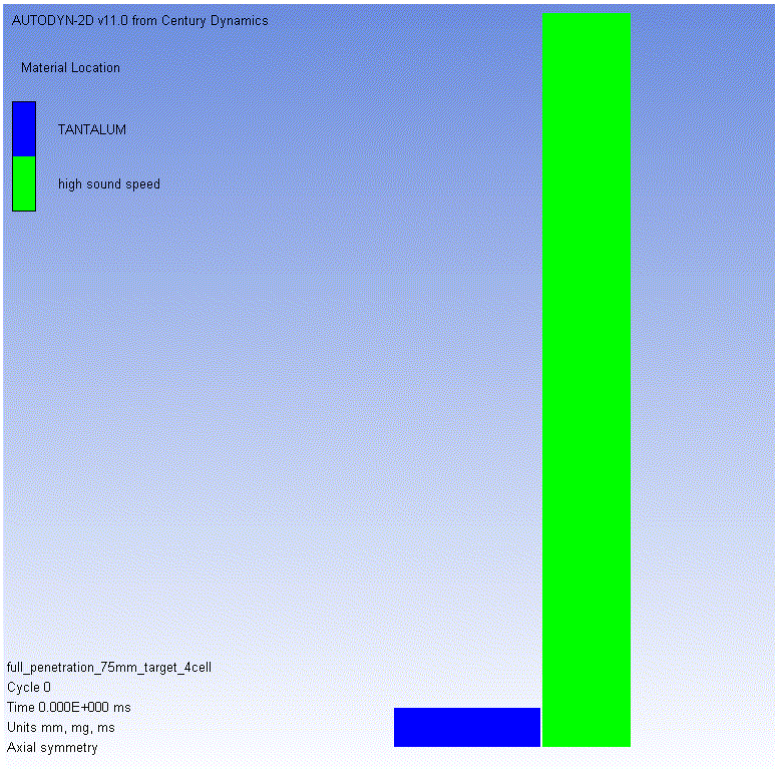

Figure 14. Lagrange 2D Axial Symmetry Setup.

A similar setup was used for the initial composite material except that the target plate is made up of three layers as shown in Figure 15. Each layer is of 3 mm thick and the first layer is the high sound speed material (green in color) followed by the low sound speed material (light blue in color) as the second layer and finally another layer of high sound speed material. Thus, making the layered target plate 9 mm thick.

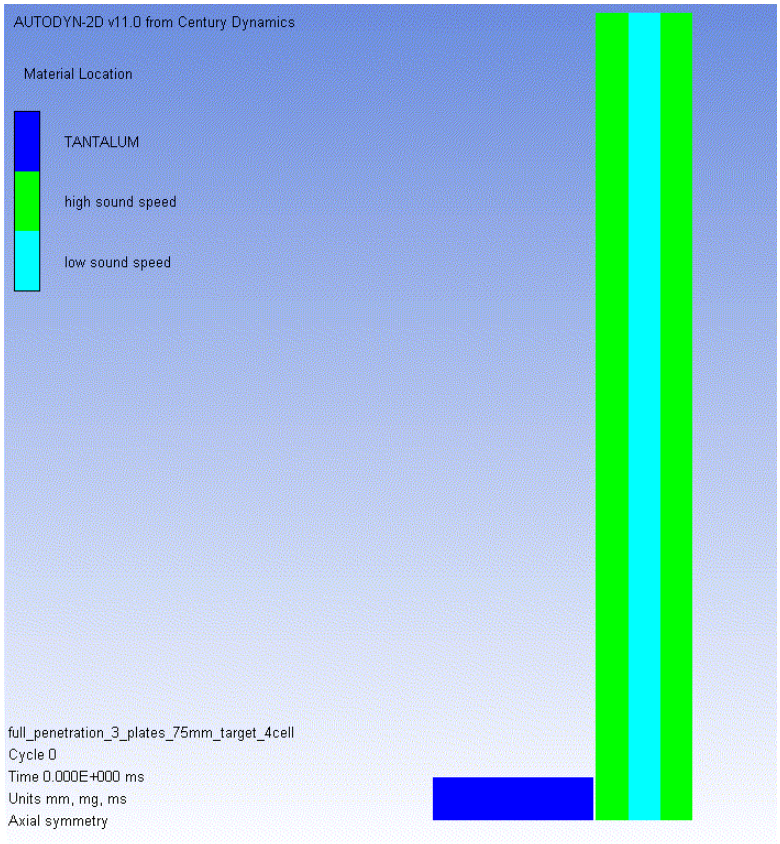

Figure 15. Layered Target Plate Simulation Setup.

For all the three simulation setups, the velocity of the projectile was set at 1000 m/s (red vector in Figure 16), and the simulation was done using four cells per mm along with seven gauges set up in the target plate as shown in Figure 16. Note that gauges are set slightly off the axis to avoid numerical artifacts that can occur there when using cylindrical geometry. The first gauge is located at the front surface of the target, while the last gauge is at the rear surface of the target with spacing of 1.5 mm between each gauge. There is an initial gap of 0.2 mm between the projectile and the target plate. Gauges were used to check wave profile shapes and to obtain stress as a function of run distance for the initial shock wave. Parameters were varied to be sure the gauges gave reasonable results for the shape of the shock waves.

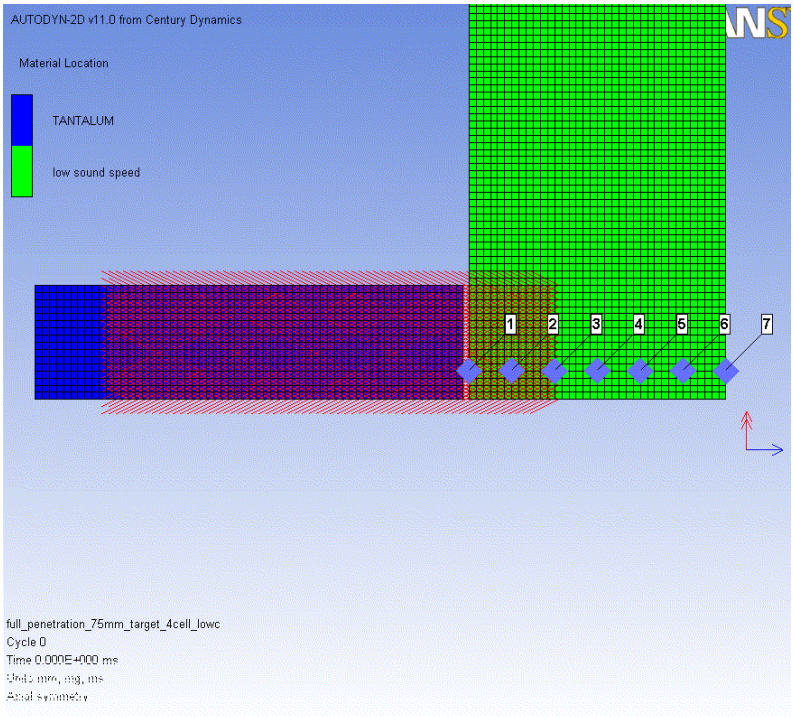

Figure 16. Zoom In of Entire Simulation Setup.

There are a variety of material models to choose from the literature for the projectile and target plate. Table 5 summarizes the equation of state (EOS), strength model, failure model, and erosion criteria for the materials used in the simulations.

Table 5. Material Properties of Wave-spreading Layer.

Equation of State	**Strength Model**	**Failure Model**	**Erosion**
Tantalum			
Shock	Steinberg Guinan	Hydro (P_{min})	Geometric Strain
C = 3414 m/s S = 1.201	G = 69 GPa Y = 0.77 GPa	σ_{spall} = - 2 GPa	Strain = 2

High Sound Speed			
Shock	Von Mises	Hydro (P_{min})	Geometric Strain
C = 15000 m/s S = 1.5	G = 30 GPa Y = 1 GPa	σ_{spall} = - 2 GPa	Strain = 2
Low Sound Speed			
Shock	Von Mises	Hydro (P_{min})	Geometric Strain
C = 1000 m/s S = 1.5	G = 30 GPa Y = 1 GPa	σ_{spall} = - 2 GPa	Strain = 2

C. SIMULATION RESULTS AND ANALYSIS

The primary objective of the simulations is to be able to better understand shock wave propagation in the defined innovative materials so as to have a better understanding of the wave-spreading layer. The ultimate goal is to be able to determine if there is enough wave spreading to lower the transmitted stress on axis. The results will be presented and discussed based on the three different setups. Using the results of these simulations, we tuned the properties of the prototype high and low sound speed materials.

1. High Sound Speed Target Plate Results and Analysis

Figure 17 shows the pressure versus time plot of the shock wave propagating through the high sound speed target plate at the various gauges. The plot clearly shows that the pressure attenuates over time as the shock wave travels through the target plate. This is due to edge releases from the impact plane propagating into the target plate laterally. This happens very quickly in this material due to the very high sound speed, and causes all of the transmitted

waves to have a triangular pressure profile. It takes about 0.54 μs after impact for the shock wave to propagate through the entire plate to reach the last gauge located at the rear surface.

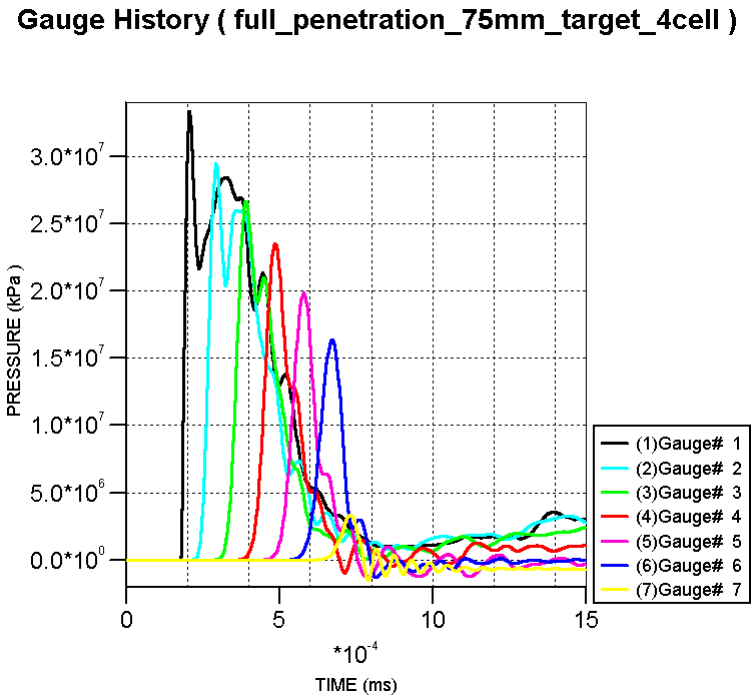

Figure 17. Pressure versus Time Plot of the High Sound Speed Target Plate.

The pressure computed by the simulation indicated an impact pressure of about 27.97 GPa at the first gauge as shown in Figure 18. Figure 19 also shows the impact pressure recorded at gauge one as about 27.97 GPa. This agrees well with pressure calculated analytically for this impact problem.

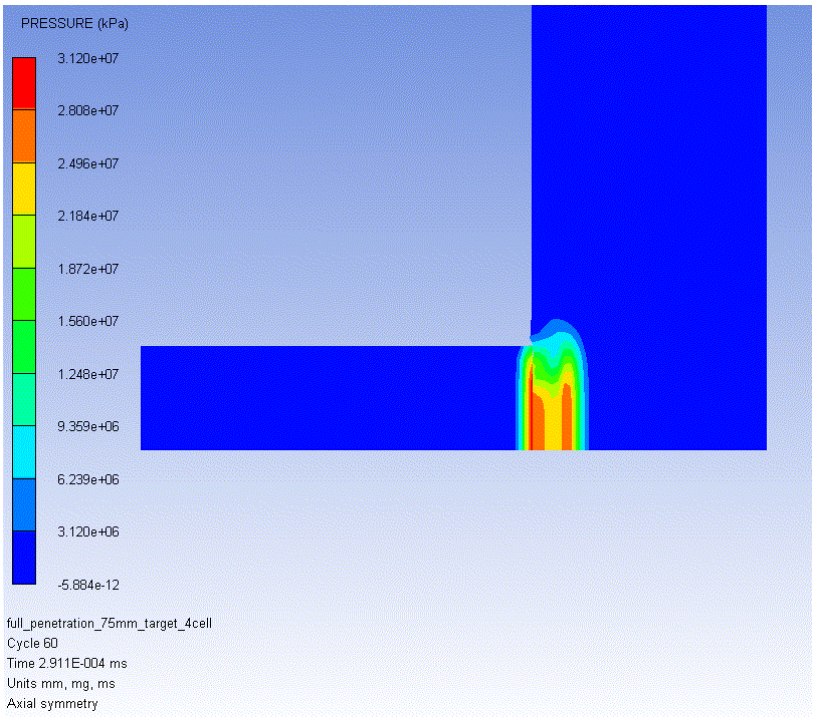

Figure 18. Pressure Plot of Gauge 1 at Initial Impact of High Sound Speed Target.

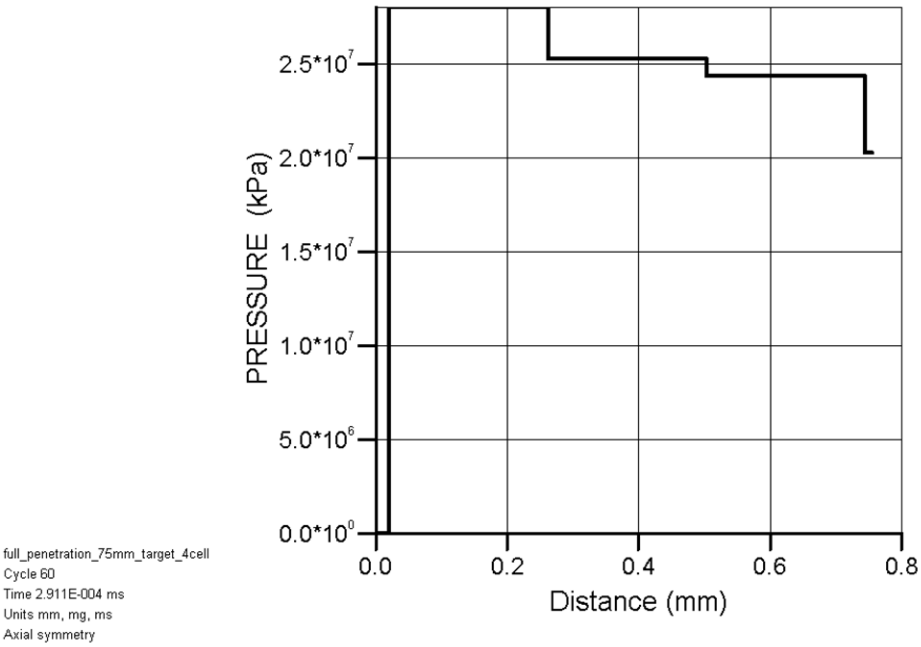

Figure 19. Impact Pressure at Gauge 1 of High Sound Speed Target.

Due to the high sound speed of the innovative material, the shock wave tends to propagate quickly through the target and at the same time, it spreads widely across the target. The pressure indicated by gauge seven at the rear surface is about 3.12 GPa as shown in Figures 20 and 21. There is a significant decrease of about 25 GPa in pressure as compared to the initial impact pressure. This simulation also yields reasonable results, giving us confidence in our problem set up.

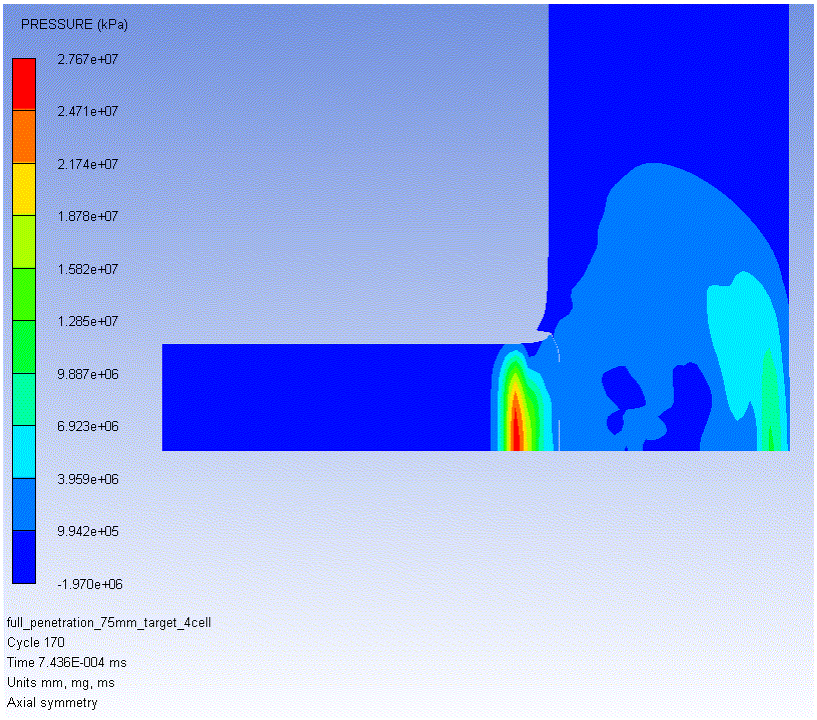

Figure 20. Pressure Plot of Gauge 7 at Rear Surface of High Sound Speed Target.

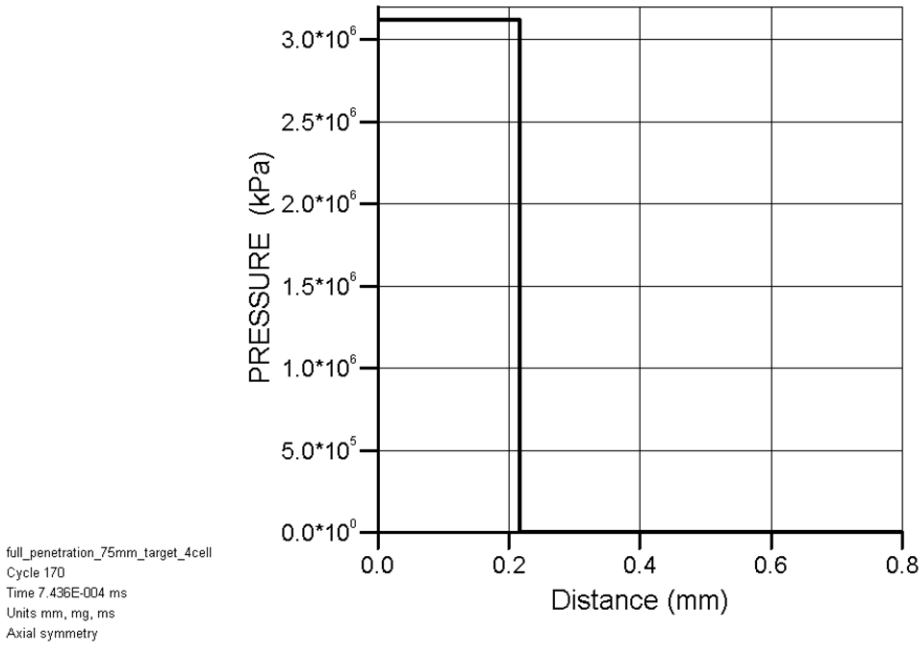

Figure 21. Rear Surface Pressure at Gauge 7 of High Sound Speed Target.

2. Low Sound Speed Target Plate Results and Analysis

A similar approach to the above was used to study properties of the low sound speed material. There are some noticeable differences in the pressure and wave speed of the shocks propagating through the target plate as compared to the high sound speed material, as expected. Figure 22 shows the pressure versus time plot of the shock wave at the various gauge locations and it shows that it takes a much longer time to propagate through the material due to the much lower sound and shock velocities. The time taken to reach the rear surface was about 5.5 μs as indicated by gauge seven (yellow in color) in Figure 22. In addition, we see (with ringing) flat top shock wave profiles for the first few gauges. This is due to the fact that edge releases take longer to reach these gauge locations than was the case for the high sound speed material.

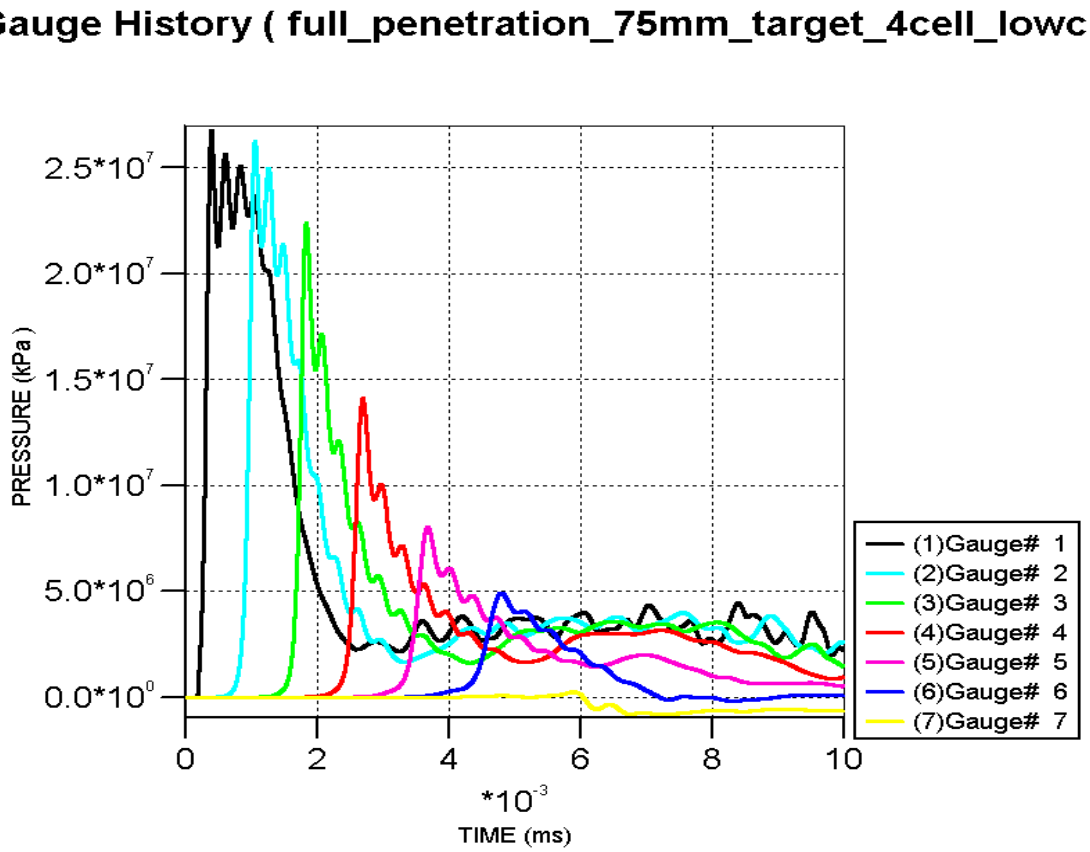

Figure 22. Pressure versus Time Plot of the Low Sound Speed Target Plate.

Due to the high density of the low sound speed material, the impact pressure simulated was about 24.25 GPa as shown in Figures 23 and 24. This impact pressure is lower than the impact pressure simulated for the high sound speed material by about 4 GPa. Figures 25 and 26 shows that the shock wave takes a noticeably longer time of 5.5 μs to reach the rear surface and the simulated pressure at the rear surface was about 0.07 GPa. The longer propagation time is caused by the slow sound speed property of the material in the through thickness. This also means that there will be less wave "spreading" laterally in this material than in the high sound speed material. The decrease in pressure between the impact pressure and the rear surface pressure is about 24 GPa.

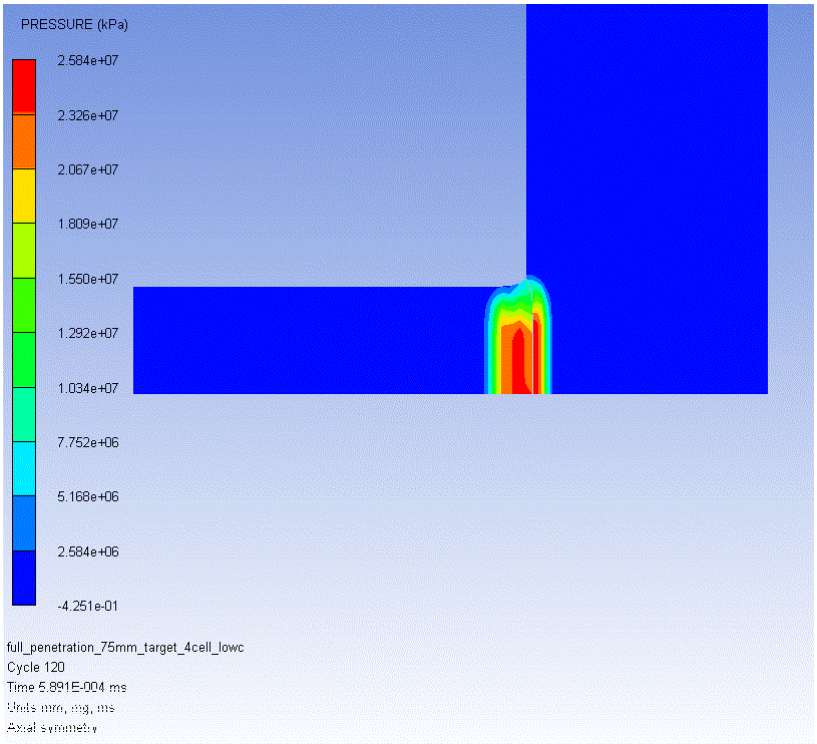

Figure 23. Pressure Plot of Gauge 1 at Initial Impact of Low Sound Speed Target.

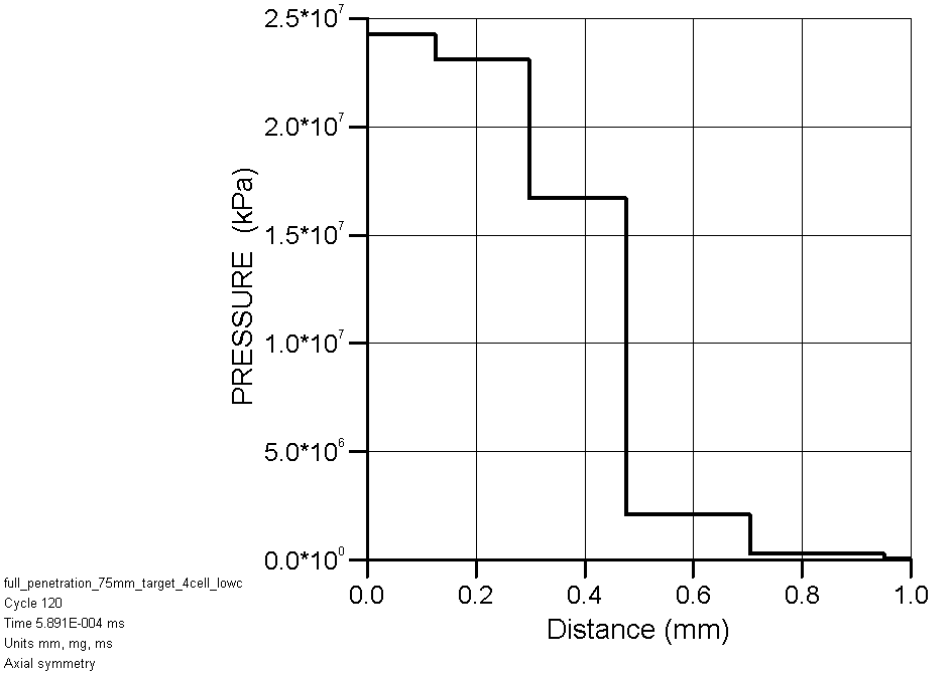

Figure 24. Impact Pressure at Gauge 1 of Low Sound Speed Target.

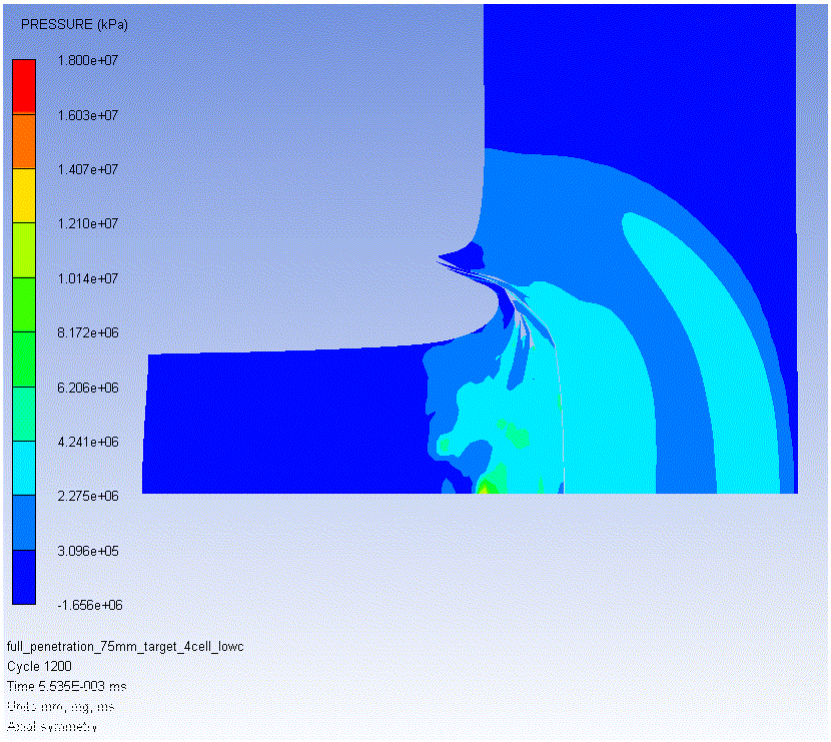

Figure 25. Pressure Plot of Gauge 7 at Rear Surface of Low Sound Speed Target.

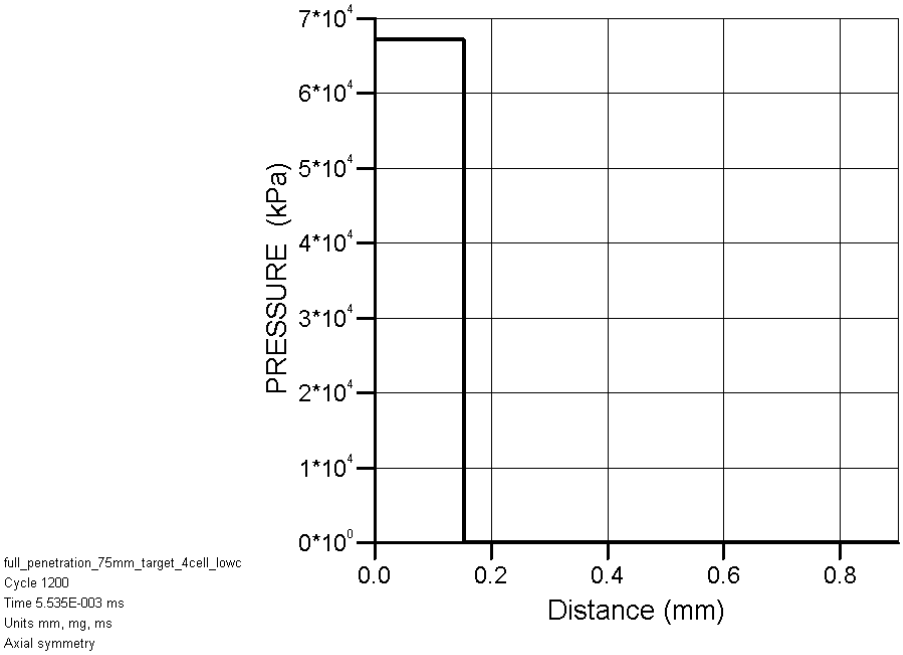

Figure 26. Rear Surface Pressure at Gauge 7 of Low Sound Speed Target.

3. Layered Target Plate Results and Analysis

The composite target plate was simulated with layers of high and low sound speed. The target plate consists of three layers; high sound speed material as first layer, low sound speed as second layer and the high sound speed as the third layer. This is the first test of the integrated response of the layered wave spreading composite material. The idea is that the through-thickness shock will be slowed by the low sound speed material, and allow time for significant wave spreading to occur in the high sound speed material. This is the desired result.

Figure 27 shows the pressure versus time plot of the shock wave propagating through the target plate. It clearly shows the significant decrease in pressure between the impact and rear surface pressure.

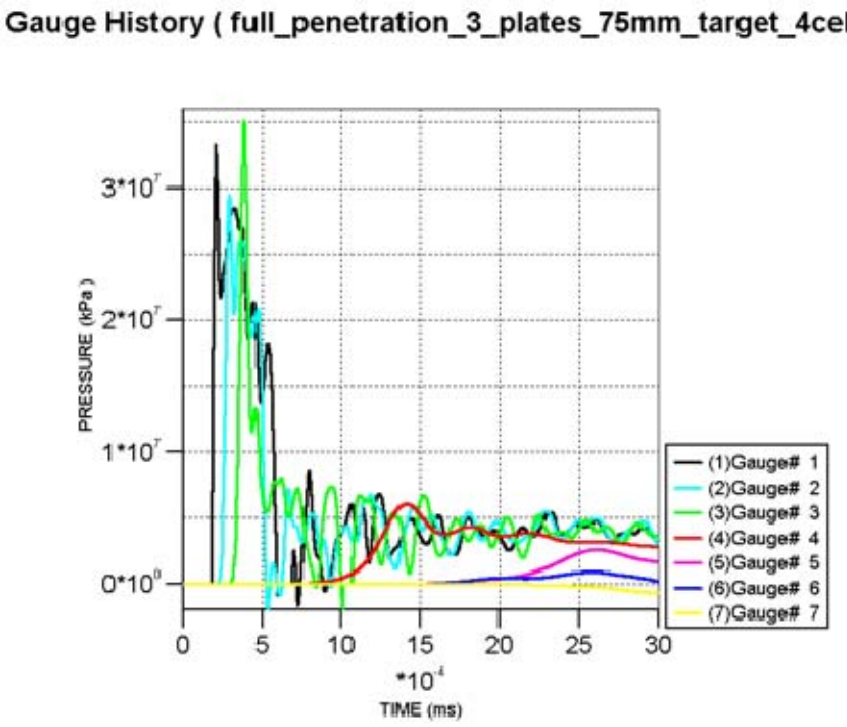

Figure 27. Pressure versus Time Plot of the Layered Target Plate.

As the first layer was made up of the high sound speed material, the simulated impact pressure was at 27.97 GPa, which is similar to the high sound speed material simulation as shown in Figures 28 and 29. However, the rear surface pressure decreased greatly to 0.02 GPa and it takes about 1.96 μs to reach the rear surface as shown in Figures 30 and 31.

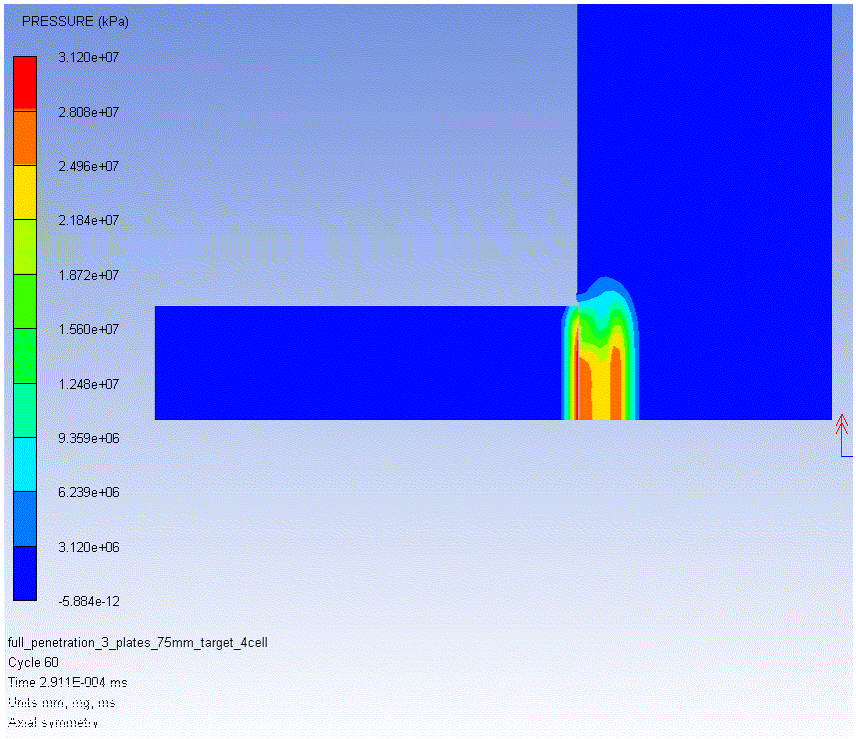

Figure 28. Pressure Plot of Gauge 1 at Initial Impact of Layered Target.

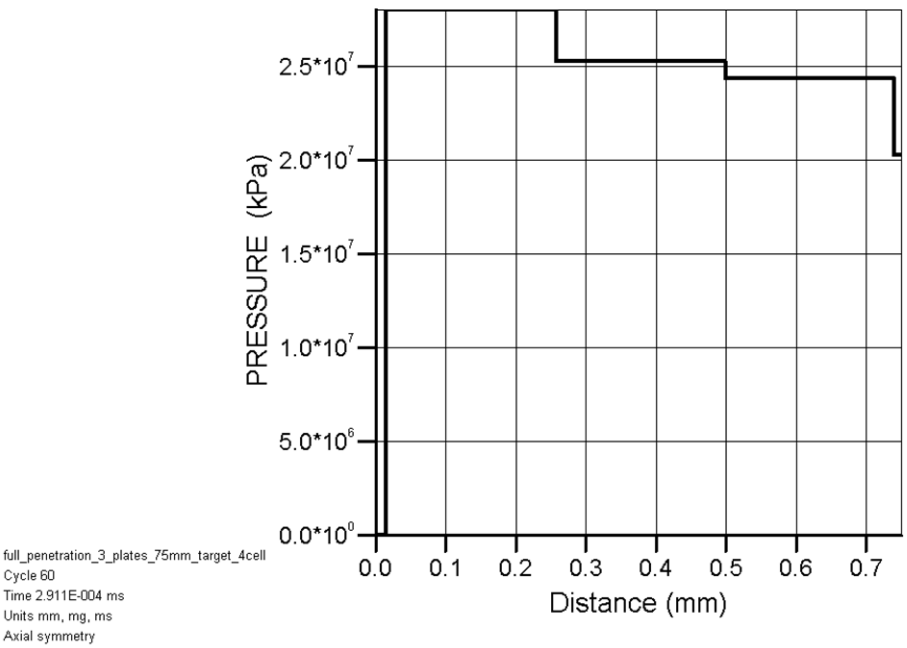

Figure 29. Impact Pressure at Gauge 1 of Layered Target.

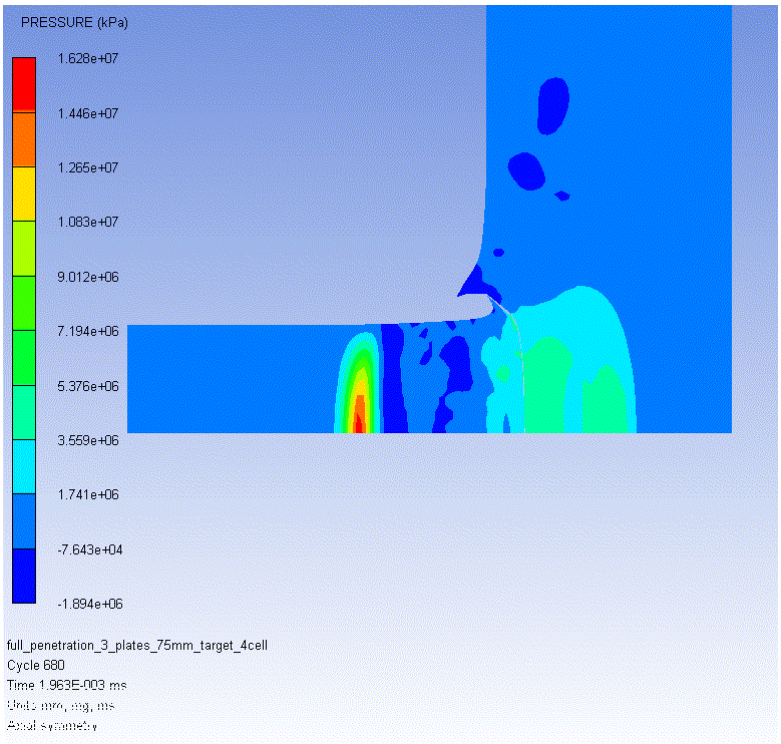

Figure 30. Pressure Plot of Gauge 7 at Rear Surface of Layered Target.

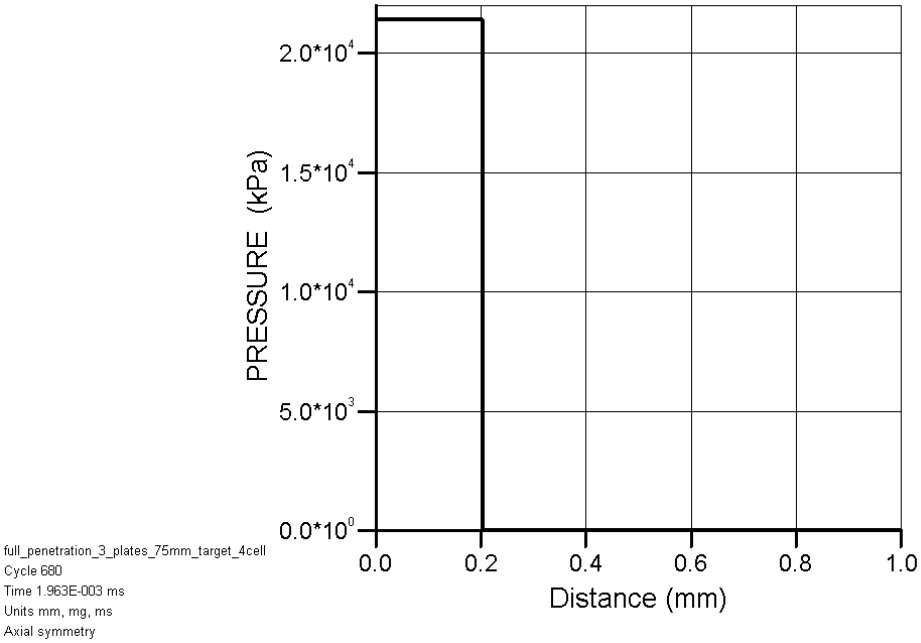

Figure 31. Rear Surface Pressure at Gauge 7 of Layered Target.

4. Comparison of Results

Table 6 summarizes the simulation results of the impact and rear surface pressure for the three simulation setups. From the simulation results, it is clearly observed that for a projectile travelling at 1000 m/s, the low sound speed material has a lower impact pressure compared to the high sound speed material due to the high density of the material. However, the high sound speed material attenuates the pressure at a much faster rate than the low sound speed material.

The layered target plate, which consists of both materials appears to be able to laterally spread out the shock wave, and at the same time attenuate the pressure more efficiently. This shows that our layered concept has the desired properties, and lead us to consider more complex layered systems.

Table 6. Simulation Results for Impact and Rear Surface Pressure.

Target Plate	**Impact Pressure (GPa)**	**Rear Surface Pressure (GPa)**
High Sound Speed	27.97	3.12
Low Sound Speed	24.25	0.07
Layered	27.97	0.02

VI. CRUSH LAYER SIMULATION STUDIES

A. INTRODUCTION

The simulation results in Chapters IV and V show that the high impedance layer and wave-spreading layer are able to attenuate and spread the shock wave efficiently. The material for the third layer would ideally be an energy absorbing material to absorb either the blast wave interactions or the impact energy of the projectile.

Porous material are known to be extremely effective in attenuating shock waves and mitigating impact pressures, so this is our initial choice for this layer. Porous materials absorb energy when the pores collapse so their internal energy, density and temperature all increase. In the process of pore collapse, the material can strongly attenuate shock waves. In additional, the kinetic energy being absorbed will be turned into heat energy as shown in Figure 32 [6] where energy is proportional to the area under a P-V curve. The waste heat is energy that is not recovered upon release of pressure. It is clear that there is much more residual energy left behind for the porous material (on the right) as compared to a full density material.

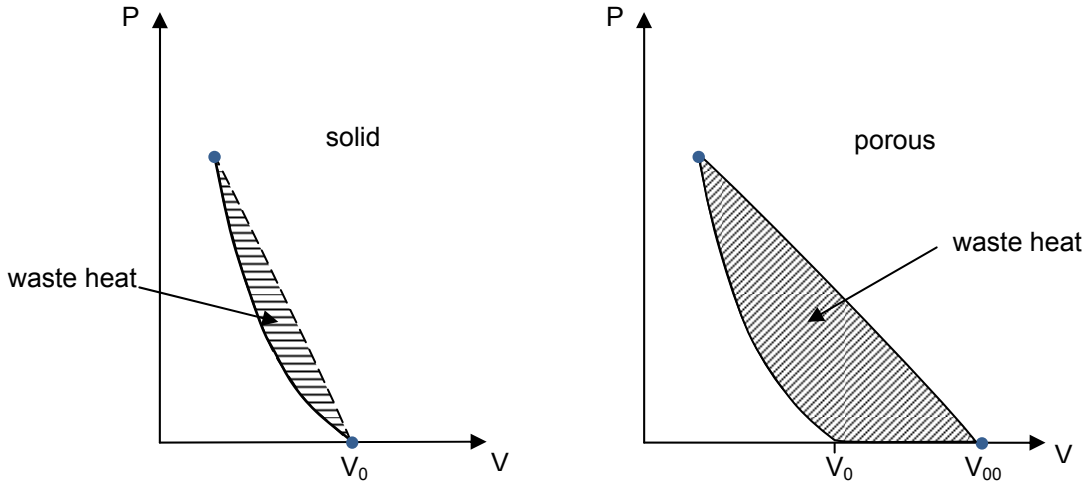

Figure 32. Comparison of Residual Energy between Solid and Porous Material.

B. SIMULATION SETUP

Similar to previous setups, the simulation is performed in 2D axial symmetry with Lagrange solvers with a tantalum projectile (dark blue in color) impacting onto a target plate. The only difference in this setup is that the material of the target plate (green in color) is made of porous 2024 aluminum. We use aluminum only to illustrate the effect; for an actual armor system it is very likely that another material would be chosen. There are no other changes to the rest of the parameters for this setup as shown in Figures 33 and 34.

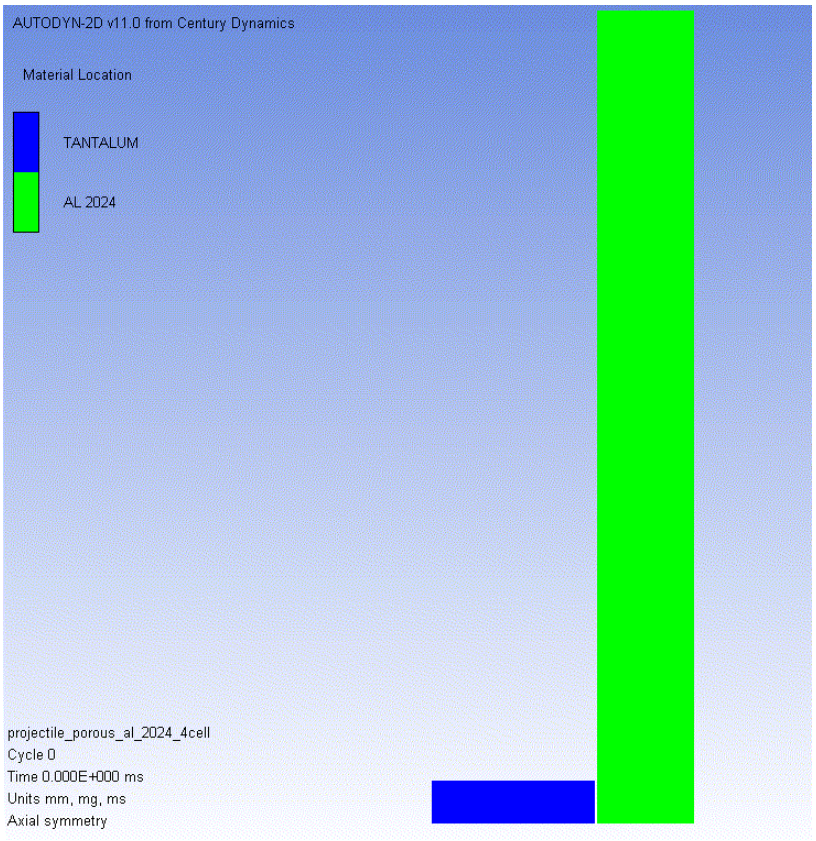

Figure 33. Crush Layer Simulation Setup.

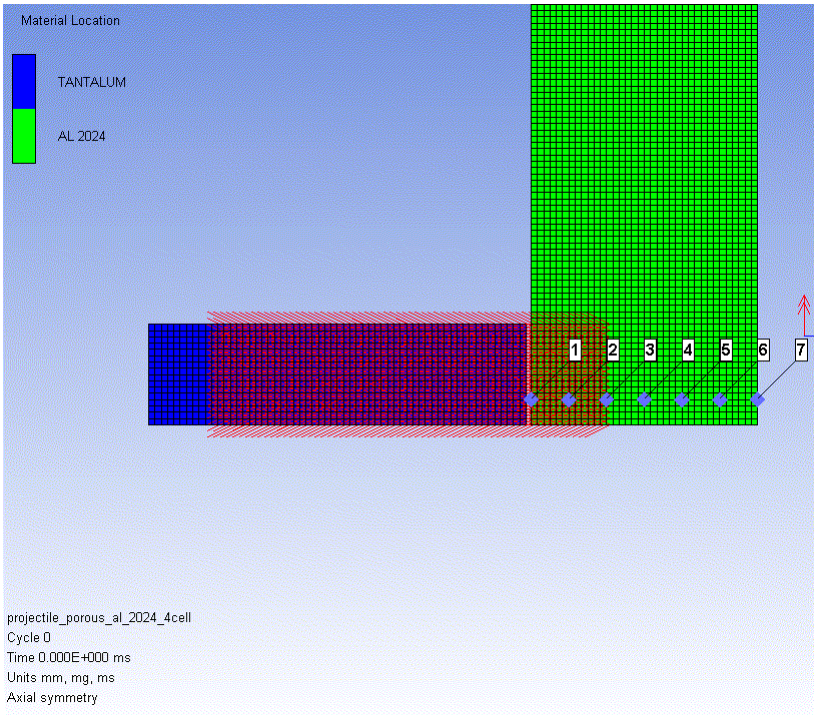

Figure 34. Zoom in of Crush Layer Simulation Setup.

There are several material models to choose from the literature research to describe the dynamic compaction of porous material. The P-α model derived by W. Herrmann [7] was selected because this model captures many of the important features of dynamic compaction while requiring only a few material parameters.

The parameters for the porous 2024 aluminum [8] were used in AUTODYN^{TM} with the P-α model. This model provides a simple way to calculate the compaction of porous materials through the use of a distention function, α. This function describes the ratio between the density of the porous material at pressure and the initial density of the solid. Table 7 summarizes the equation of state (EOS), strength model, failure model, and erosion criteria for the materials used in the simulations.

Table 7. Material Properties of Crush Layer Simulation.

Equation of State	Strength Model	Failure Model	Erosion
Tantalum			
Shock	Steinberg Guinan	Hydro (P_{min})	Geometric Strain
C = 3414 m/s S = 1.201	G = 69 GPa Y = 0.77 GPa	σ_{spall} = - 2 GPa	Strain = 2
Porous 2024 Aluminum			
P-α	Von Mises	Hydro (P_{min})	Geometric Strain
ρ_{porous} = 2.16 g/cm^3 C_{porous} = 3130 m/s P_E = 0.08 GPa P_s = 0.7GPa	G = 11.4 GPa Y = 0.08 GPa	σ_{spall} = - 2 GPa	Strain = 2

C. SIMULATION RESULTS AND ANALYSIS

Figure 35 shows the pressure versus time plot of the shock wave at the various gauges. Due to the porosity of the 2024 aluminum, the plot in Figures 36 and 37 clearly shows that the initial impact pressure is at about 6.25 GPa which is very low as compared to the impact pressure of the first two layers. Even though porous material is more efficient in attenuating shock wave, it is not a good material for the first or second layer due its poor resistance to penetration because of its low density. Therefore, it is placed as the third layer to absorb energy.

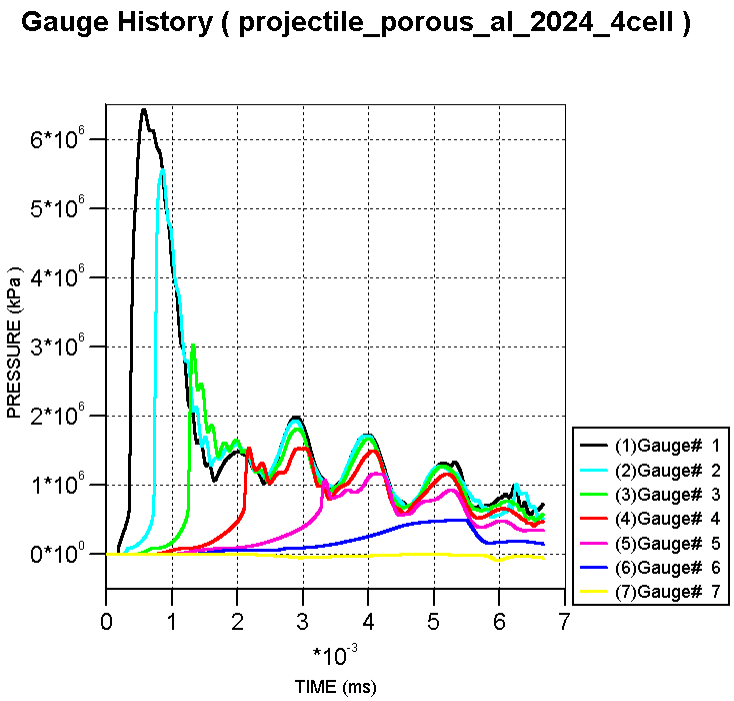

Figure 35. Pressure versus Time Plot of the Crush Layer.

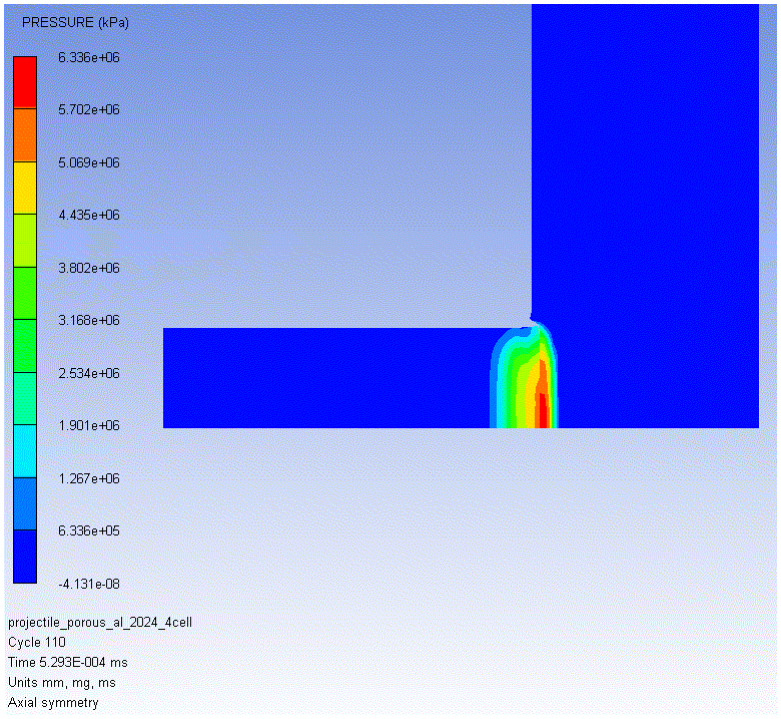

Figure 36. Pressure Plot of Gauge 1 at Initial Impact of Crush Layer.

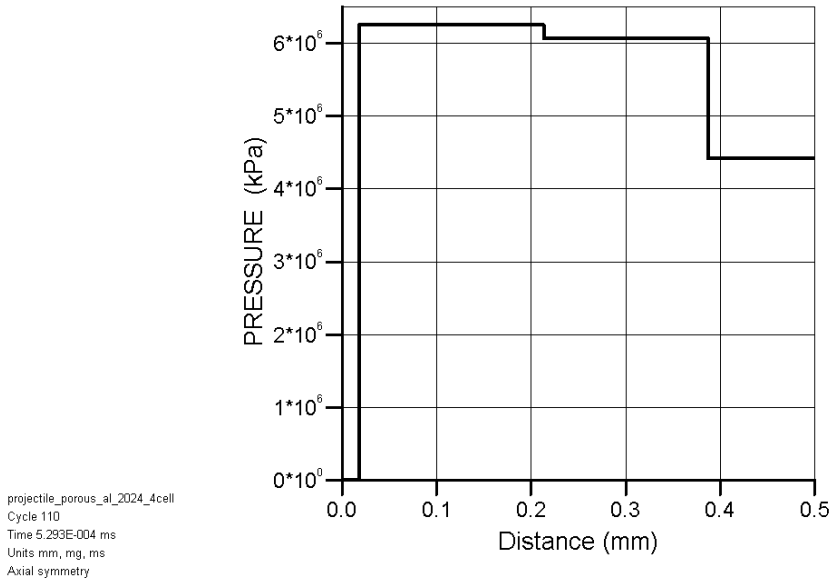

Figure 37. Impact Pressure at Gauge 1 of Crush Layer.

The rear surface pressure simulated and recorded by gauge six is about 0.42 GPa as shown in Figures 38 and 39. In Figure 39, it is clearly shown that the shock wave continues to attenuate rapidly to zero due to the porosity of the material.

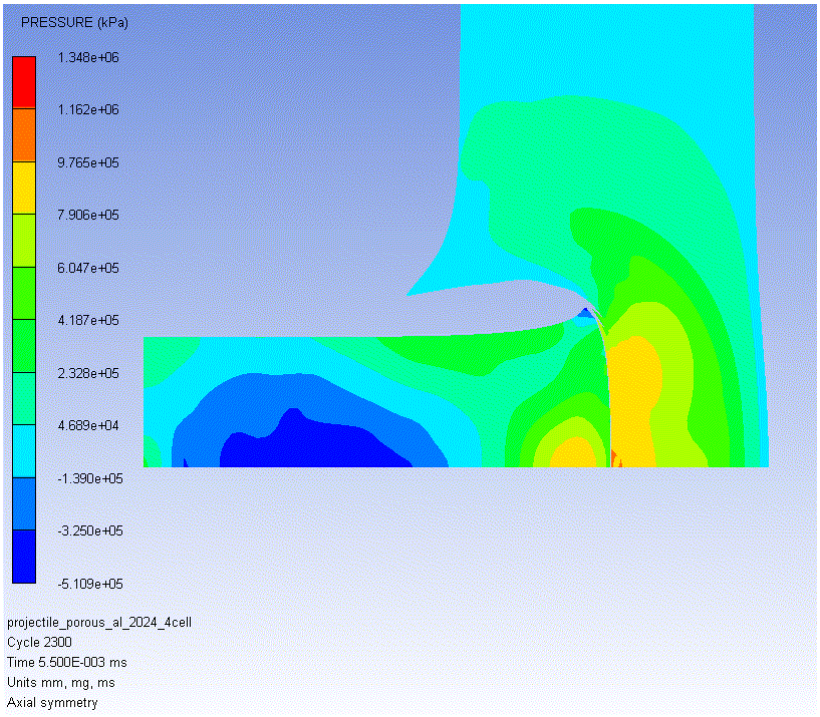

Figure 38. Pressure Plot of Gauge 6 at Rear Surface of Crush Layer.

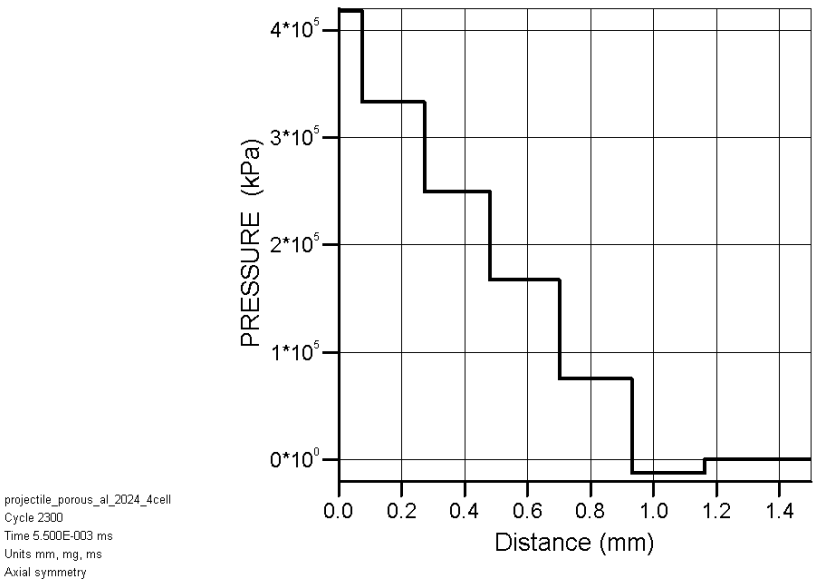

Figure 39. Impact Pressure at Gauge 6 of Crush Layer.

THIS PAGE INTENTIONALLY LEFT BLANK

VII. FINAL STOPPING LAYER SIMULATION STUDIES

A. INTRODUCTION

The simulated results for the first three layers show potential penetration resistant to projectile impact. As such, the idea for the last layer is to provide a final stopping layer, which also serves as an inner comfort layer for the personnel; in addition this layer can also serve to wick moisture from the user. The material chosen for this layer should be light, flexible and penetration resistant, and be able to provide some ventilation for the user. For vehicle protection armor, this material would be chosen just for its ability to resist penetration.

B. SIMULATION SETUP

The simulation setup in the final layer is no difference from the previous setups as shown in Figure 40.

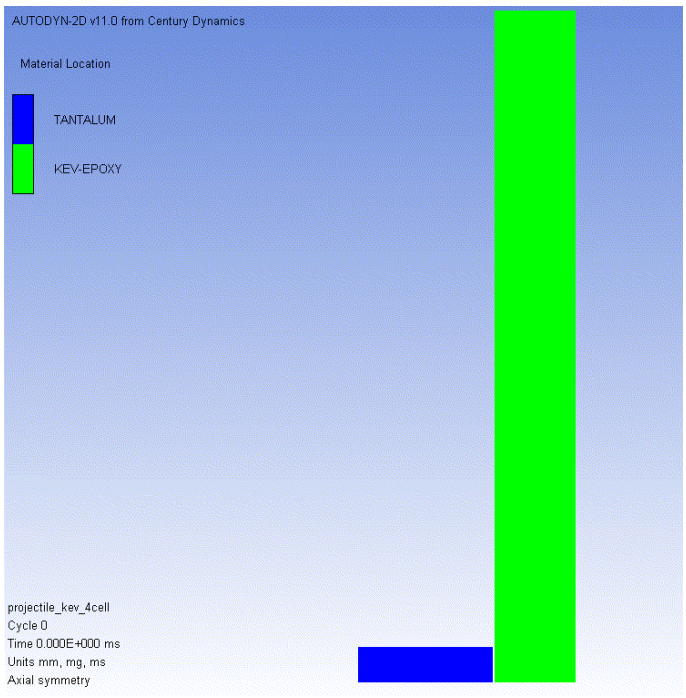

Figure 40. Final Layer Simulation Setup.

The only difference between this and previous simulations is the selection of the material for the target plate. The material selected for the target from the material library in AUTODYN™ is the Kev-Epoxy material (green in color) as shown in Figure 41. This material was selected because it is known to be light and penetration resistant; its material model parameters are shown in Table 8. Kevlar™ is an aramid fiber (aramid = aromatic polyamide) developed by DuPont in the 1960's. It is highly oriented with its maximum strength in the fiber direction, and relies upon fundamental chemical bonds for its strength. When made into a woven material it is known to have high resistance to penetration and is used in helmets, vests, and other protective equipment. It is a good first choice for this layer.

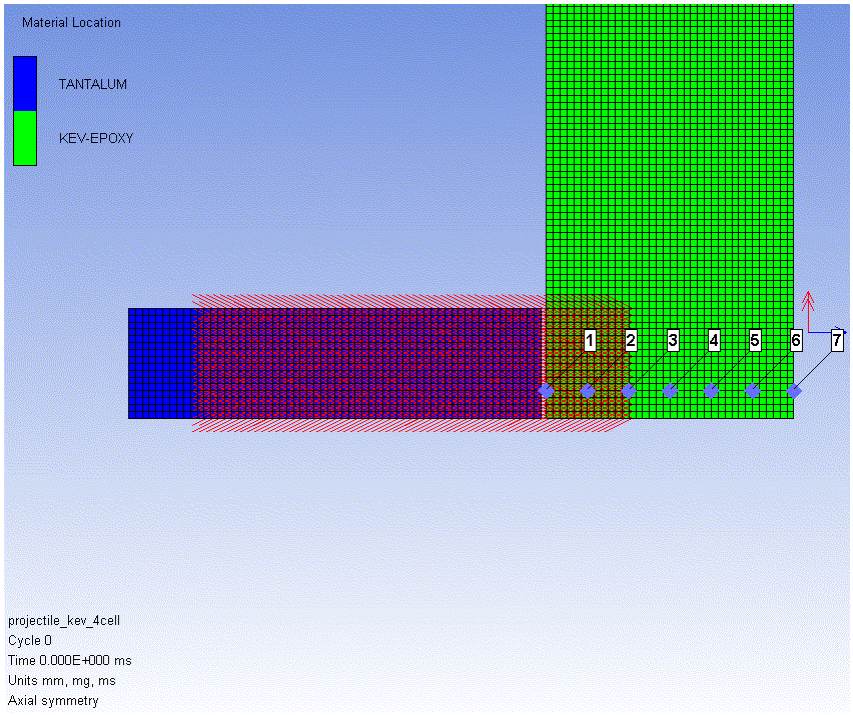

Figure 41. Zoom in of Final Layer Simulation Setup.

Table 8. Material Properties of Final Layer Simulation.

Equation of State	Strength Model	Failure Model	Erosion
Tantalum			
Shock	Steinberg Guinan	Hydro (P_{min})	Geometric Strain
C = 3414 m/s S = 1.201	G = 69 GPa Y = 0.77 GPa	σ_{spall} = - 2 GPa	Strain = 2
Kev-Epoxy			
Ortho	Elastic	Material Stress/Strain	Geometric Strain
C_{11} = 3.425 GPa C_{22} = 13.5 GPa C_{33} = 13.5 GPa C_{12} =1.14 GPa C_{23} = 1.2 GPa C_{31} = 1.14 GPa G_{12} = 1GPa G_{23} = 1 GPa G_{31} = 1 GPa	G = 1 GPa	$\sigma_{11} = 1 \times 10^{23}$ Pa $\sigma_{22} = 1 \times 10^{23}$ Pa $\sigma_{33} = 1 \times 10^{23}$ Pa $\sigma_{12} = 1 \times 10^{23}$ Pa $\sigma_{23} = 1.01 \times 10^{23}$ Pa $\sigma_{31} = 1.01 \times 10^{23}$ Pa $\varepsilon_{11} = 0.01$ $\varepsilon_{22} = 0.08$ $\varepsilon_{33} = 0.08$ $\varepsilon_{12} = 1 \times 10^{20}$ $\varepsilon_{23} = 1.01 \times 10^{20}$ $\varepsilon_{31} = 1.01 \times 10^{20}$	Strain = 2

C. SIMULATION RESULTS AND ANALYSIS

The pressure versus time plot of the shock wave at the various gauge locations is as shown in Figure 42. The initial impact pressure recorded is about 4.98 GPa as shown in Figures 43 and 44. This impact pressure attenuates to about 0.85 GPa when it reaches the rear surface of the target as shown in Figures 45 and 46.

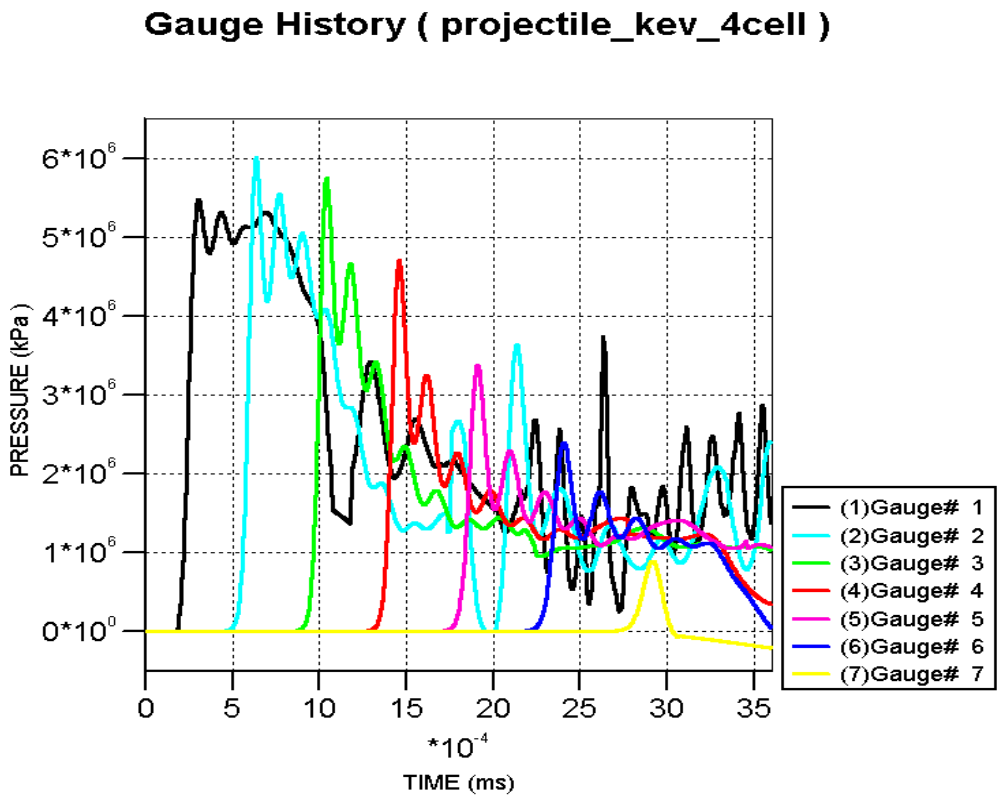

Figure 42. Pressure versus Time Plot of the Final Layer.

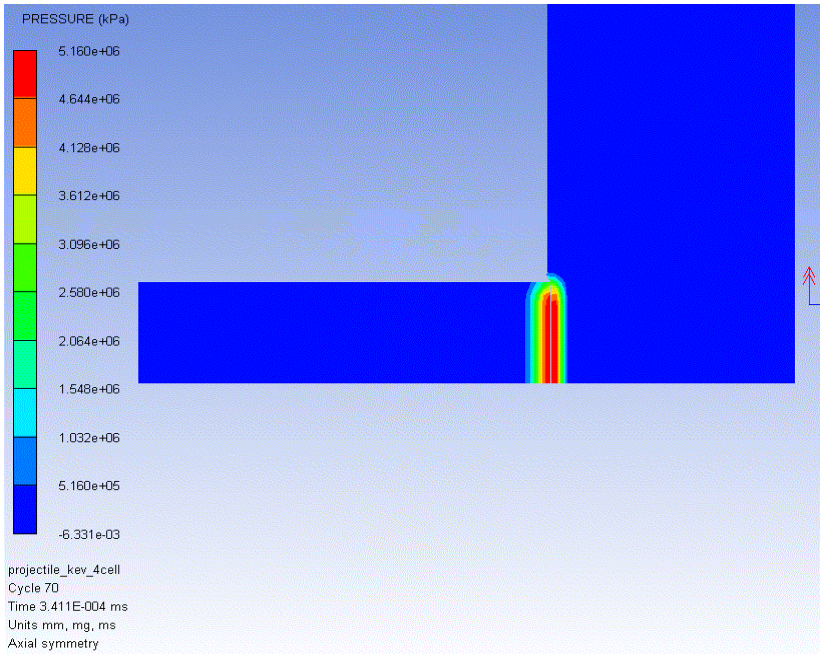

Figure 43. Pressure Plot of Gauge 1 at Initial Impact of Final Layer.

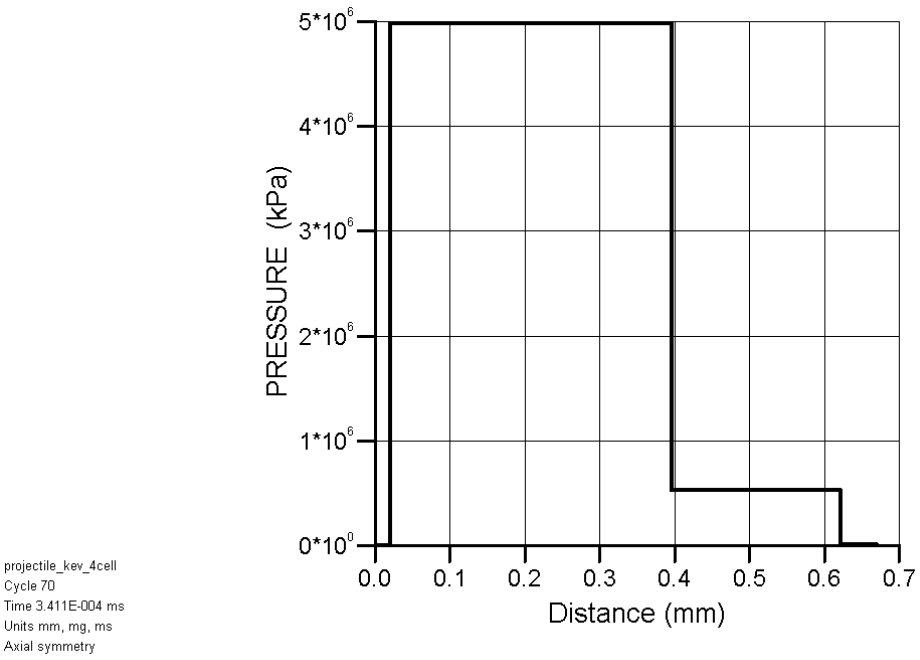

Figure 44. Impact Pressure at Gauge 1 of Final Layer.

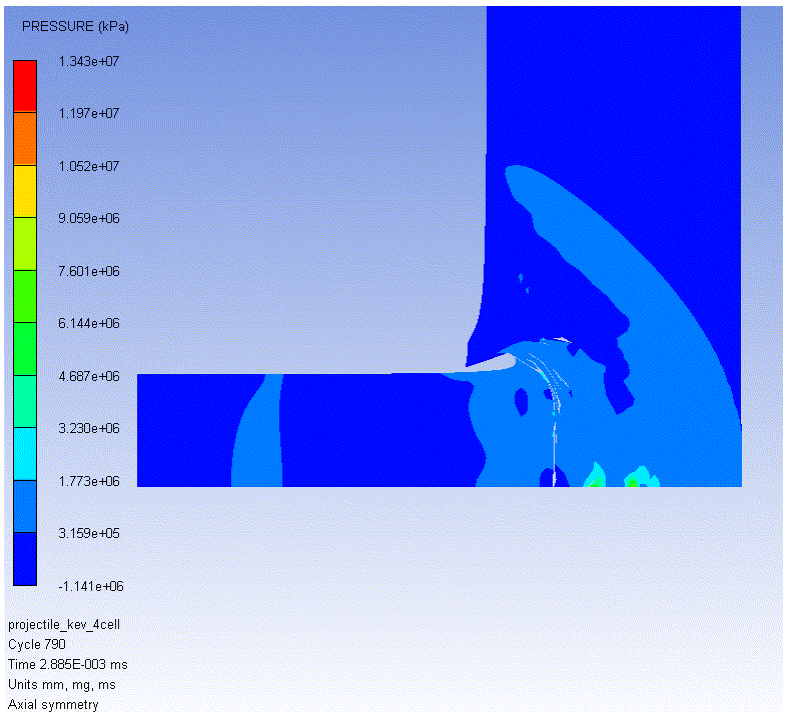

Figure 45. Pressure Plot of Gauge 7 at Rear Surface of Final Layer.

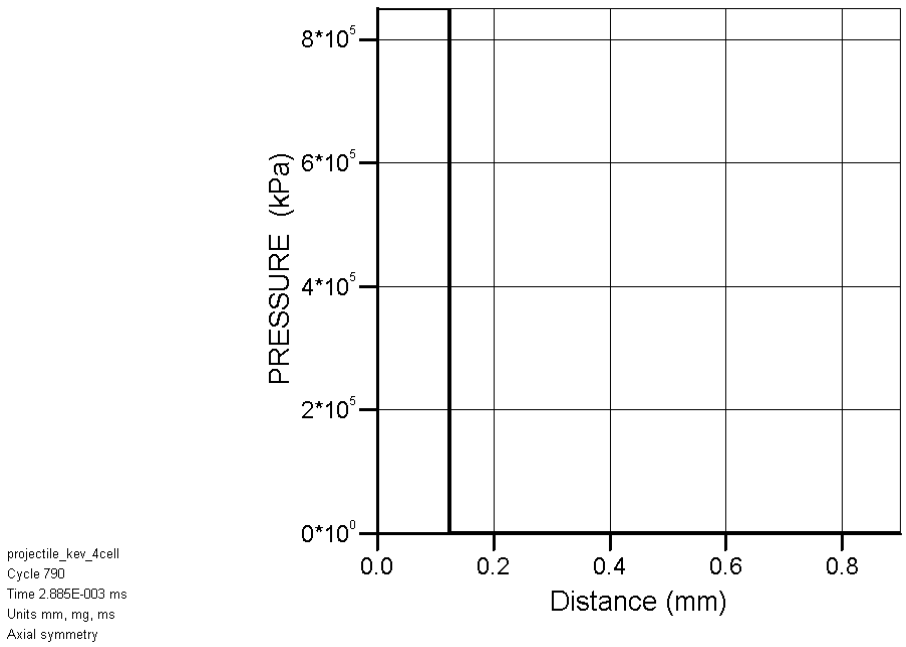

Figure 46. Impact Pressure at Gauge 7 of Final Layer.

VIII. LAYERED TARGET PLATE SIMULATION STUDIES

A. INTRODUCTION

The motivation for this research is to study new armor concepts through different materials using the understanding of the fundamental of shock physics. The focus will be on the fragment and projectiles penetration physics.

The simulations performed in the previous chapters for the various layers show promising results in terms of penetration resistance and pressure attenuation, and show that our simulations were well behaved and yielded physically realistic results. Because no one material can have all the correct properties to mitigate against both blast effects and the localized impact from fragments or projectiles, we use a layered model in which each layer has specific desirable properties. Therefore, with the simulation results obtained from the previous chapters it is now possible to test the concept of a four layered target plate in mitigating blast wave and resisting projectile penetration.

This will be the first time that the four different layers are integrated together as a complete layered target plate to test the penetration resistance to projectile impact. For comparison purposes, a steel target plate of the same thickness was chosen as the baseline material to do direct comparison with the layered target plate.

B. SIMULATION SETUP

We used two different simulation setups in order to be able to make comparisons between performance of the steel plate and the layered plate. Both simulation setups use 2D Lagrange axial symmetry. The only difference is in the material for the target plate.

Figure 47 shows the simulation setup for the steel target. The projectile (dark blue in color) has a length of 20 mm and a radius of 4 mm simulating the size of a 7.62 mm projectile. The steel target plate (green in color) has a thickness of 16 mm.

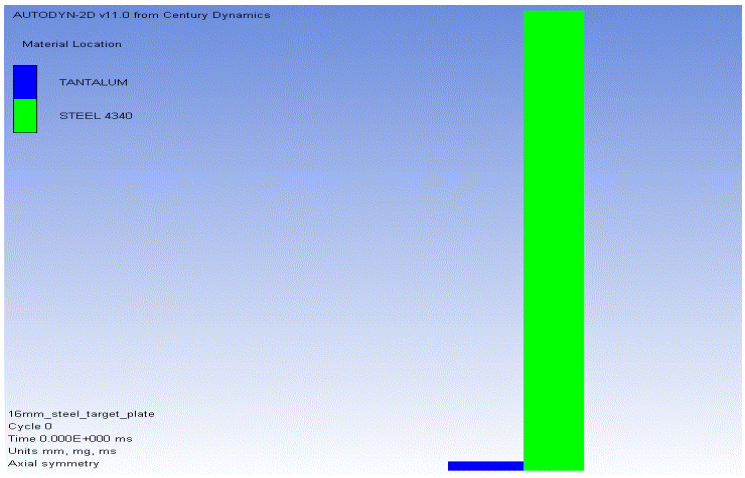

Figure 47. Steel Target Plate Simulation Setup.

Table 9 summarizes the equation of state (EOS), strength model, failure model, and erosion criteria for the materials used in the steel plate simulation.

Table 9. Material Properties of Steel Target Plate Simulation.

Equation of State	**Strength Model**	**Failure Model**	**Erosion**
Steel 4340			
Linear	Johnson Cook	Johnson Cook	Geometric Strain
K = 159 GPa	G = 77 GPa Y = 0.79 GPa	D1 = 0.05 D2 = 3.44 D3 = -2.12 D4 = 0.002 D5 = 0.61	Strain = 2

The four-layered target plate as shown in Figure 48 is a combination of the four layers that were studied in the previous chapters. The first layer is the high impedance layer (pink in color) made of tantalum and has a thickness of 1 mm.

The wave-spreading layer (green and light blue in color) made of composite materials of high and low sound speed is the second layer and has a thickness of 9 mm. The porous 2024 aluminum (red in color) forms the third layer with a thickness of 4 mm and the fourth layer is the final stopping layer (yellow in color) made of Kev-epoxy has a thickness of 2 mm. The target plate has a total thickness of 16mm.

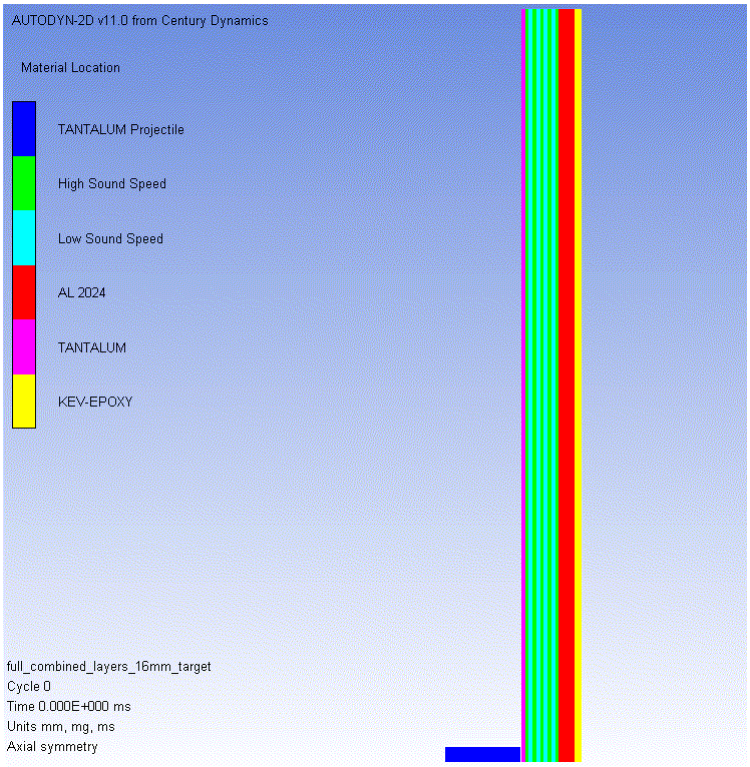

Figure 48. Layered Target Plate Simulation Setup.

Figure 49 shows that there are 17 gauges set within the layered target plate with spacing of 1 mm between each gauge. The velocity of the projectile is 1000 m/s and the simulation was performed with a zoning of four cells per mm. The material models used in this simulation setup are the same as the previous setups for the various layers except that the yield stress of the high and low sound speed materials has been changed to 3 GPa instead of 1 GPa. It was

changed to a higher yield stress value so as to test on the penetration resistance of the layered plate with material strength at a relatively high value.

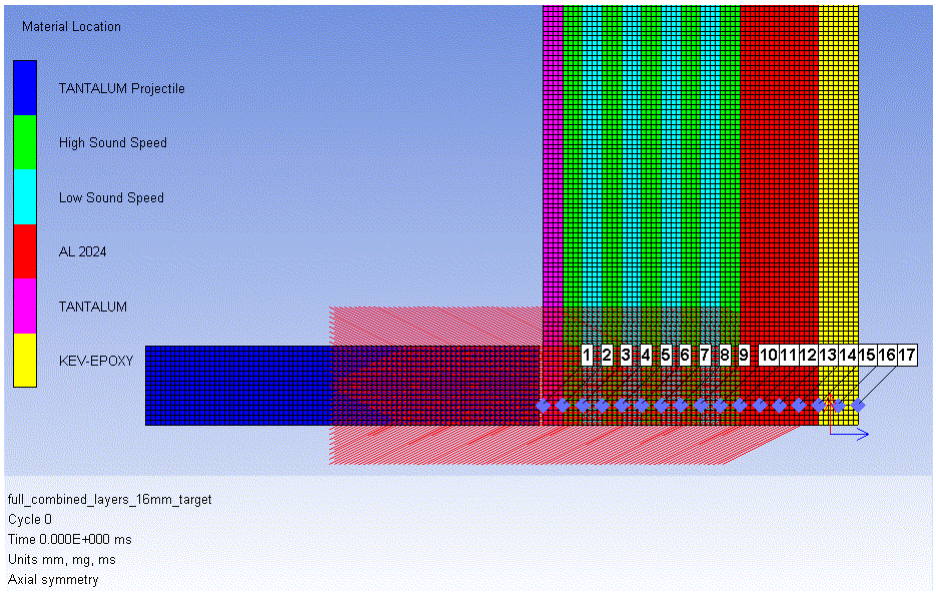

Figure 49. Zoom in of Layered Target Plate Simulation Setup.

C. SIMULATION RESULTS AND ANALYSIS

A steel plate was chosen to be the baseline material for comparison with the layered target plate. The simulated results for both the steel plate and the layered target will be presented and discussed.

1. Steel Target Plate Results and Analysis

Figure 50 shows the pressure versus time plot of the shock wave within the steel plate. The initial impact pressure is about 23.18 GPa as shown in Figures 51 and 52. As the shock wave propagates through the target plate, the pressure attenuates over time to about 0.09 GPa at the rear surface as shown in Figures 53 and 54.

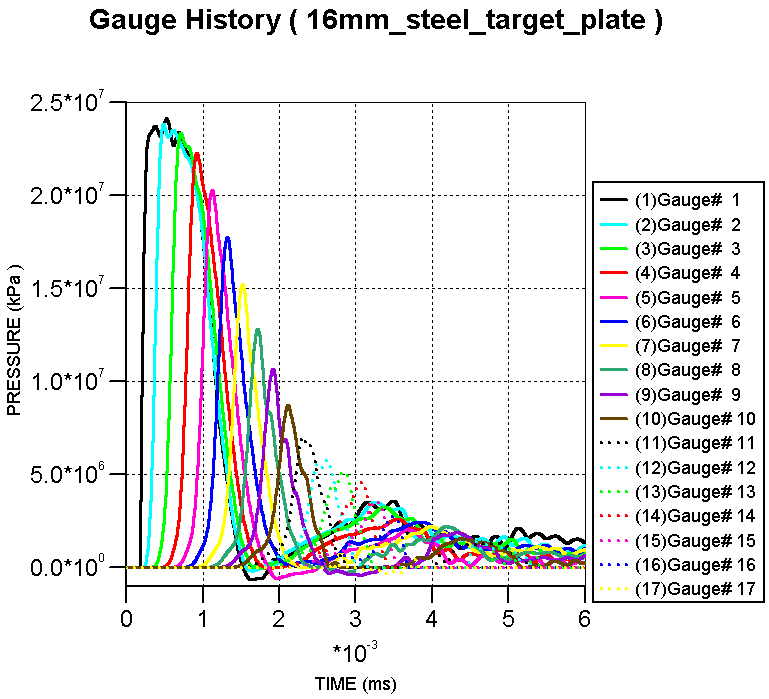

Figure 50. Pressure versus Time Plot of the Steel Target Plate.

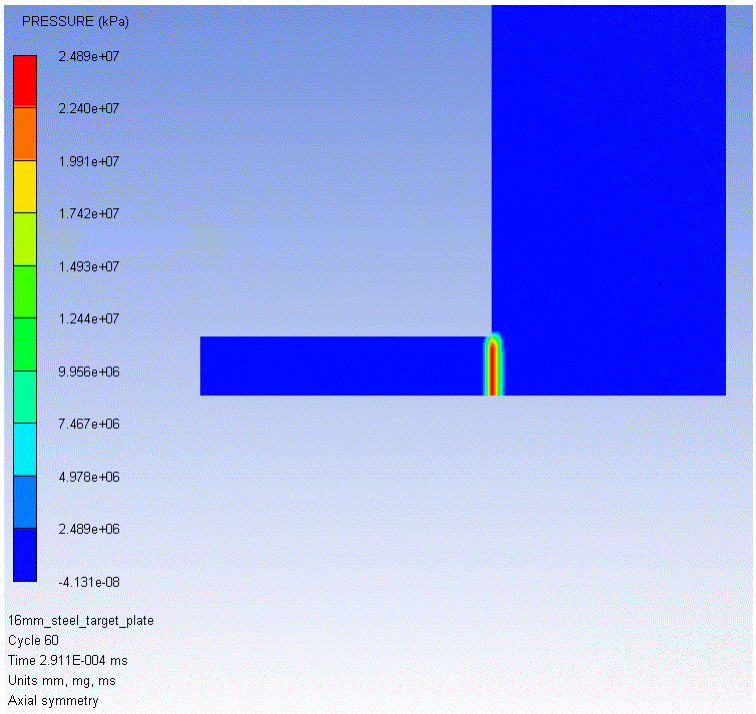

Figure 51. Pressure Plot of Gauge 1 at Initial Impact of Steel Target Plate.

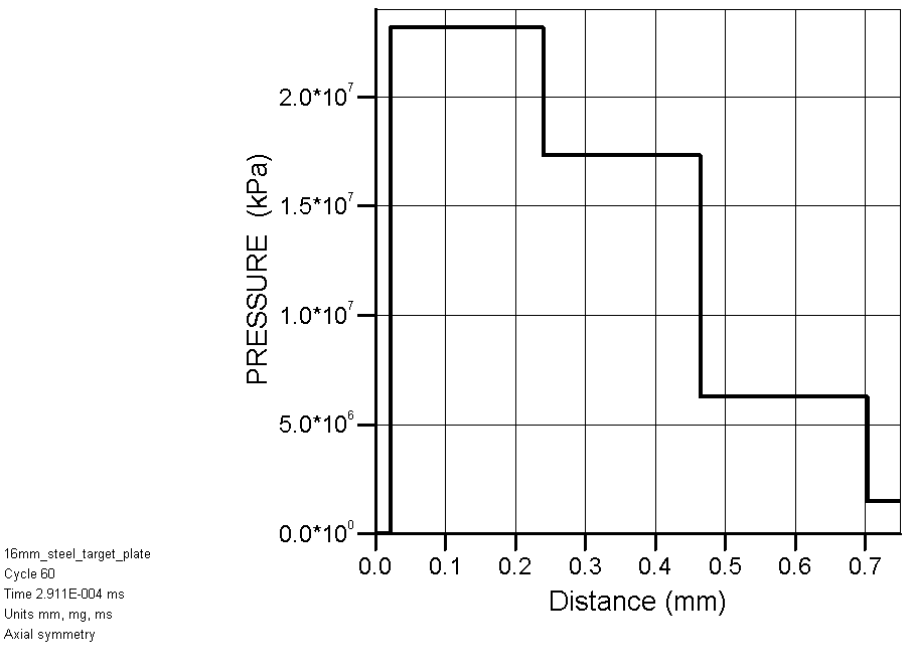

Figure 52. Impact Pressure at Gauge 1 of Steel Target Plate.

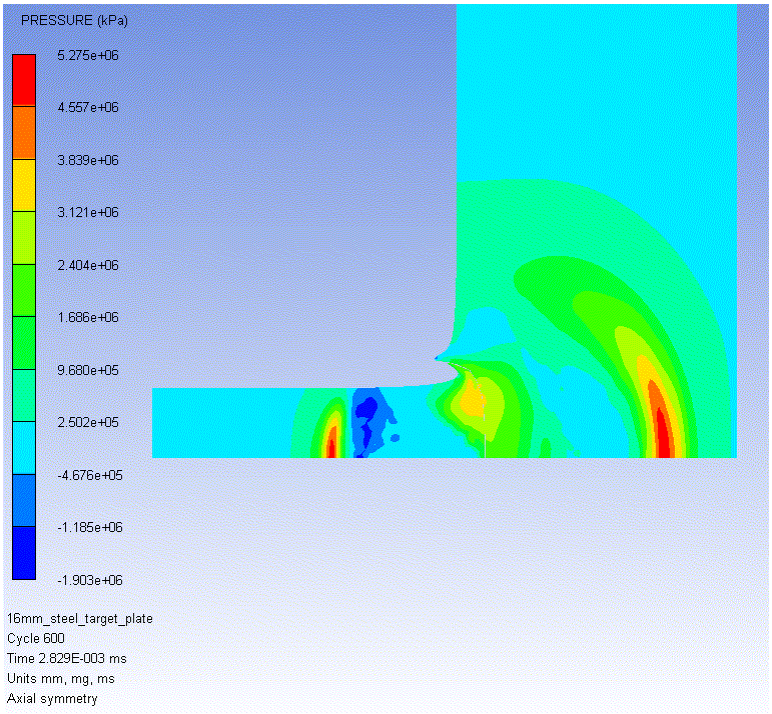

Figure 53. Pressure Plot of Gauge 17 at Rear Surface of Steel Target Plate.

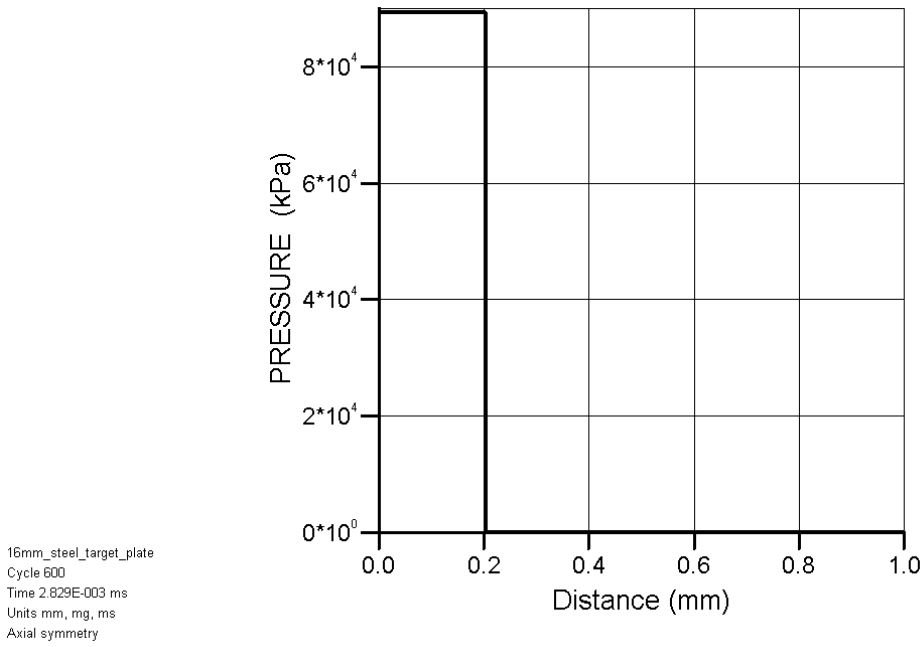

Figure 54. Impact Pressure at Gauge 17 of Steel Target Plate.

2. Layered Target Plate Results and Analysis

The pressure versus time plot of the shock wave traveling through the layered plate is as shown in Figure 55. From the plot, it can be seen that the impact pressure is at a much higher value than the steel plate but it attenuates the pressure more efficiently as compared to the steel plate. This is largely due to the combination of the desired properties of the various layers forming the layered plate.

The initial impact pressure simulated was about 33.9 GPa as shown in Figures 56 and 57. However, this pressure was attenuated to just about 0.007 GPa when it reaches the rear surface of the layered target plate assembly as shown in Figures 58 and 59.

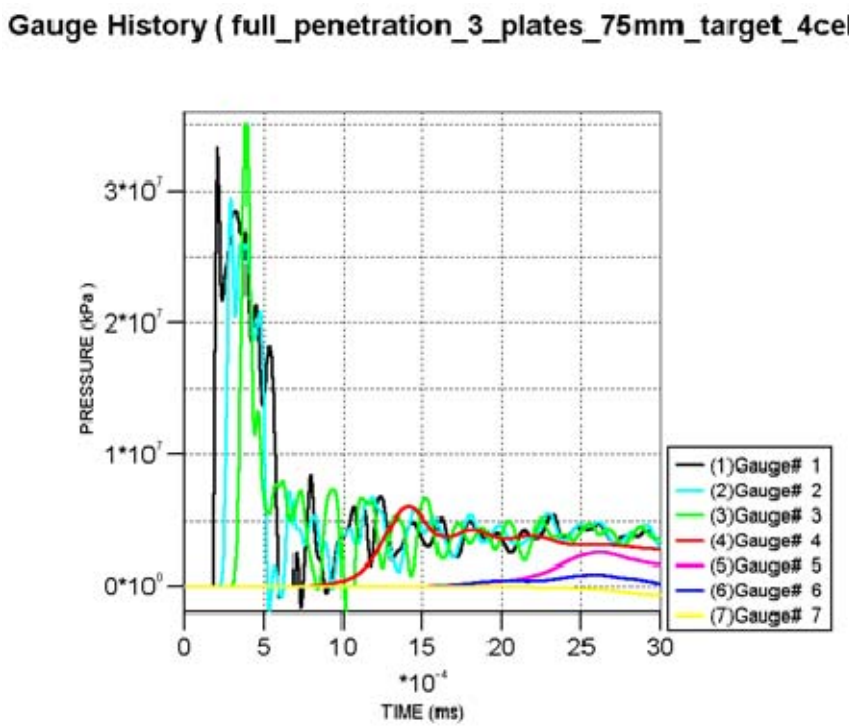

Figure 55. Pressure versus Time Plot of the Layered Target Plate.

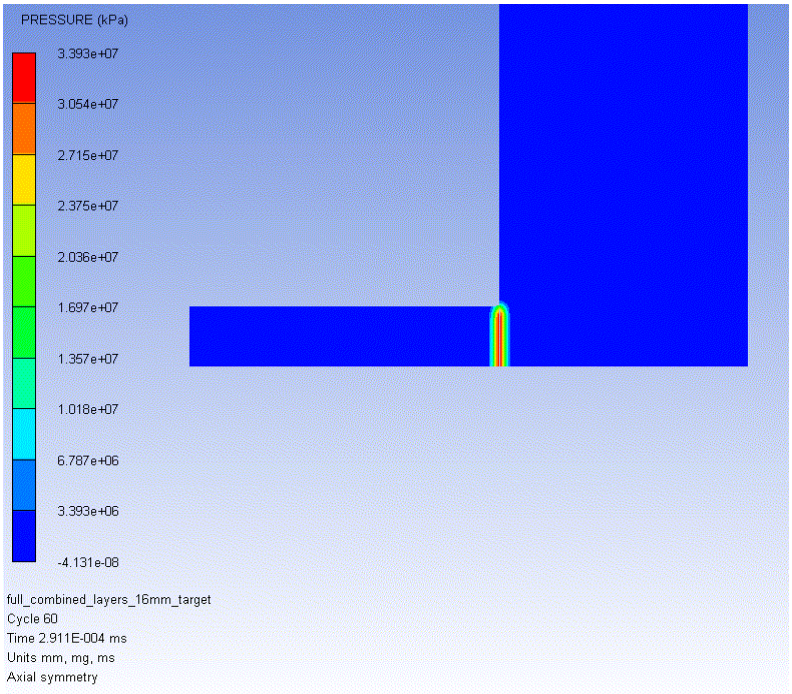

Figure 56. Pressure Plot of Gauge 1 at Initial Impact of Layered Target Plate.

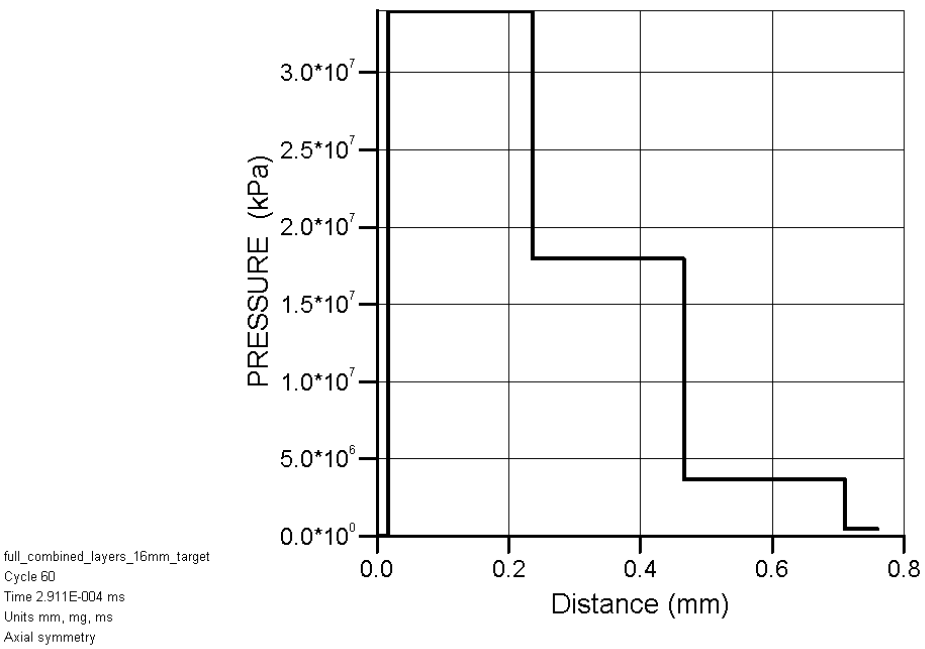

Figure 57. Impact Pressure at Gauge 1 of Layered Target Plate.

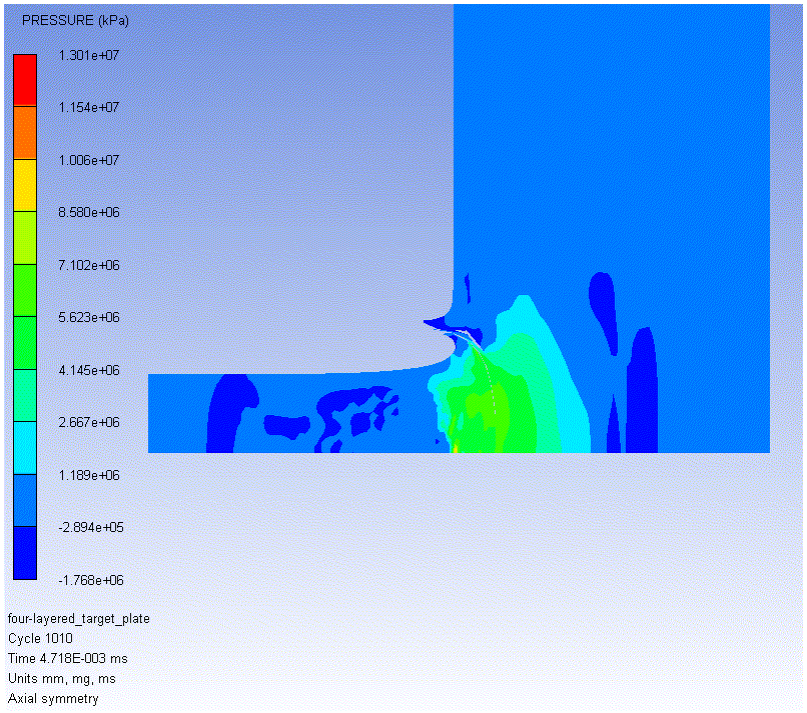

Figure 58. Pressure Plot of Gauge 17 at Rear Surface of Layered Target Plate.

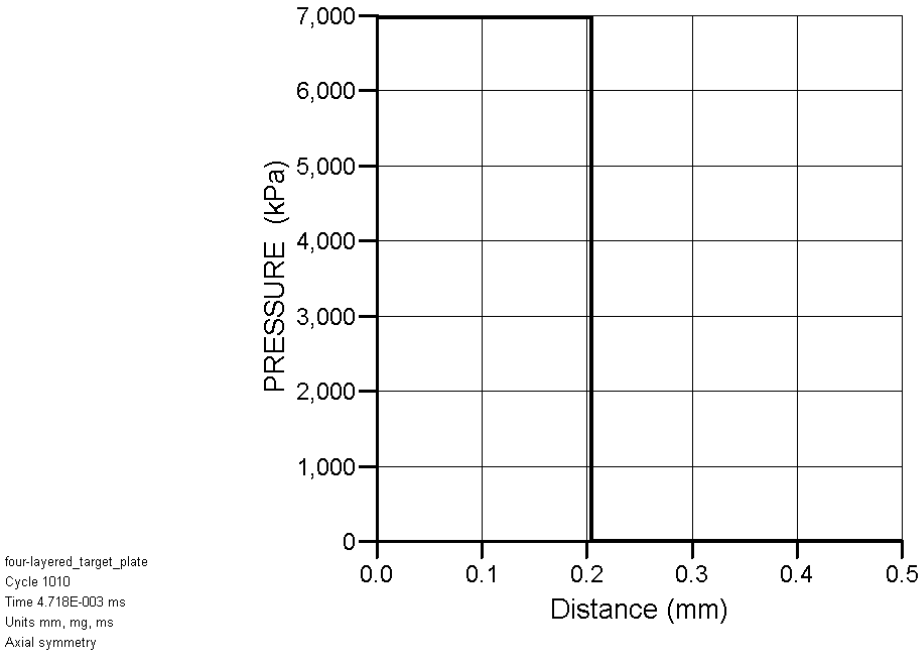

Figure 59. Impact Pressure at Gauge 17 of Layered Target Plate.

3. Comparison of Penetration Effects

Figure 60 shows the time it takes for the projectile to penetrate the steel target plate completely. It takes about 64 μs for the projectile to completely penetrate through the 16 mm steel plate. The velocity of the projectile at the time of complete penetration is about 760 m/s as shown in Figure 61. The projectile is still traveling at a relatively high speed as compared to the initial velocity of 1000 m/s. This means that considerable damage would still be sustained by any material on the rear surface of this plate.

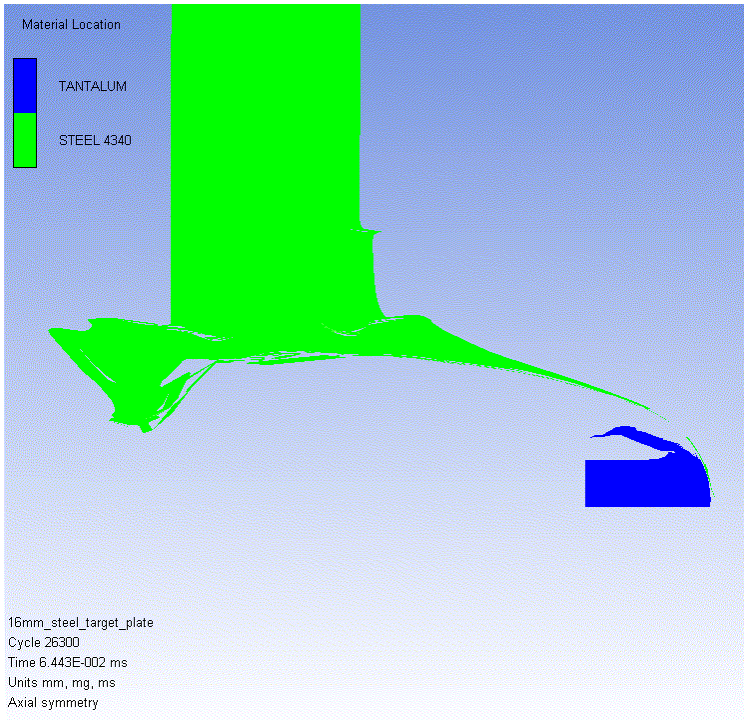

Figure 60. Penetration Depth of Steel Target Plate.

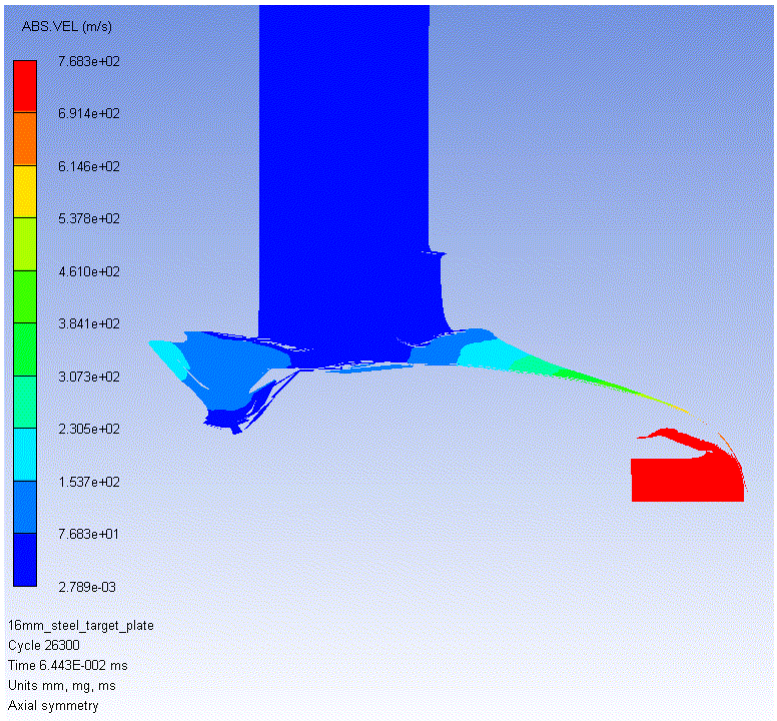

Figure 61. Final Velocity of Projectile of Steel Target Plate.

Figure 62 shows the penetration depth in the layered target using the same projectile traveling at the same initial velocity of 1000 m/s and at the same time of 64 μs. The only difference is that the target plate is composed of the layered materials instead of steel. It clearly shows that the penetration effect of the projectile is significantly reduced. The same projectile only managed to penetrate about 8 – 10 mm into the layered target plate. The other noticeable difference is that the velocity of the projectile at the same time of 64 μs had been reduced to less than 37 m/s as shown in Figure 63. The lack of penetration and reduction in velocity is largely due to the combination of the wave-spreading layer and porous layer of the composite layered target plate.

In fact, it was observed that the velocity of the projectile was reduced to about 41 m/s at an earlier time of about 45 μs as shown in Figure 64. This shows that the projectile will not have enough kinetic energy to penetrate through the layered target plate completely.

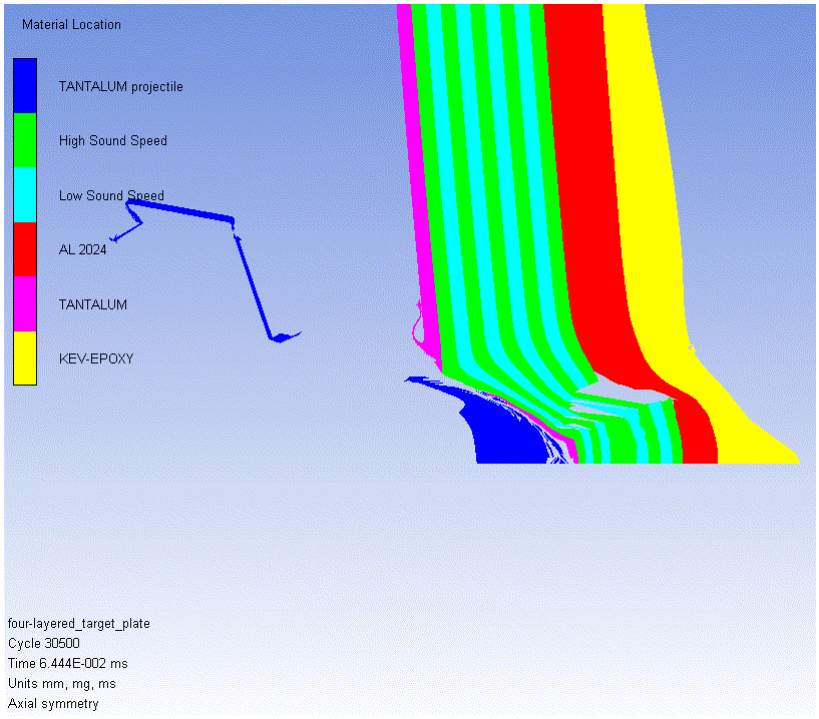

Figure 62. Penetration Depth of Layered Target Plate.

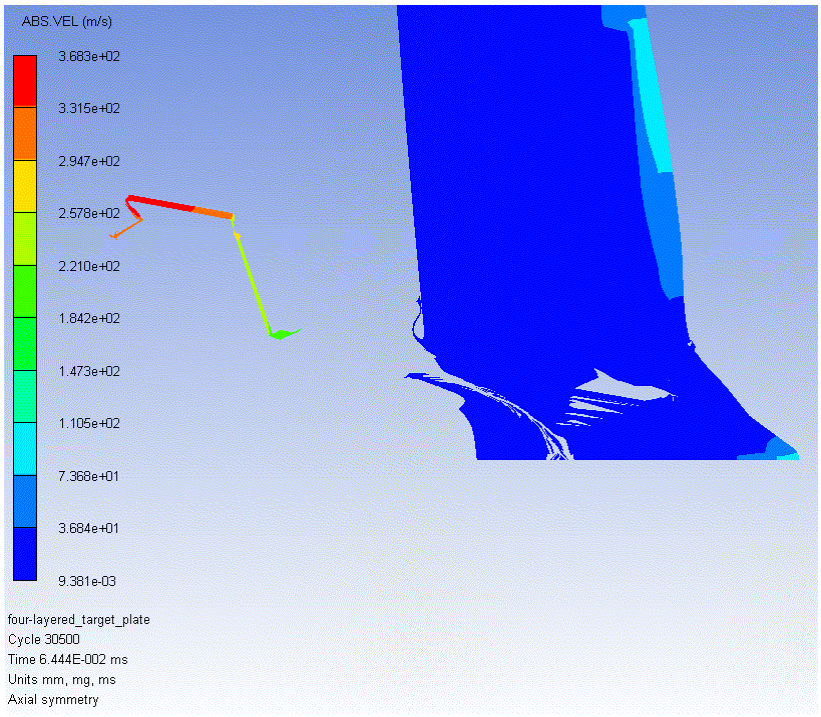

Figure 63. Final Velocity of Projectile of Layered Target Plate.

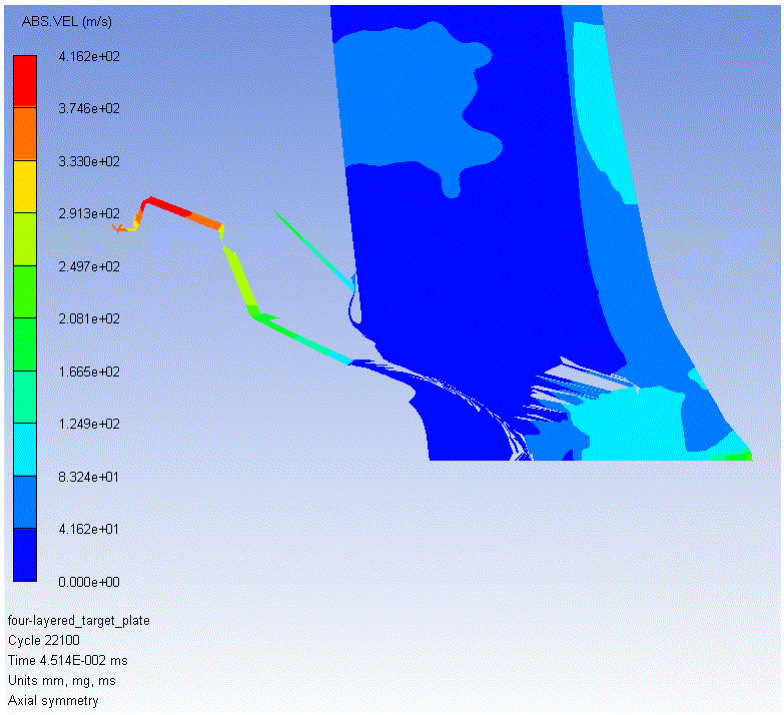

Figure 64. Velocity of Projectile of Layered Target Plate at 45μs.

In addition, a comparison is done between the densities of the two plates. The density of the steel plate is 7.83 g/cm^3 and the average density of the layered plate is 7.89 g/cm^3. Despite the many different layers of materials used for the layered plate, the densities for both plates are very close to one another. Table 10 summarizes the key differences between the two target plates.

Table 10. Comparison between Steel and Layered Target Plate.

Target Plate	**Impact Pressure (GPa)**	**Rear Surface Pressure (GPa)**	**Penetration Depth (mm)**	**Final Velocity (m/s)**	**Density (g/cm^3)**
Steel	23.18 GPa	0.09 GPa	16	760	7.83
Layered	33.9 GPa	0.007 GPa	8 – 10	> 37	7.89

IX. CONCLUSIONS AND RECOMMENDATIONS

A. CONCLUSIONS

The main objective for the research is to use fundamental shock physics methods to explore existing or new materials for a new armor concept that is robust to penetration. The main innovative concept is the combination of an anisotropic wave-spreading layer with a porous material to convert kinetic energy into heat. We wished to compare performance of such a composite material with that of a typical armor material (steel).

Simulation studies performed in previous chapters show promising results in resistance to penetration and in attenuating shock waves. With these results in hand, we can in further studies refine the approach and do similar calculations using real materials. The individual properties of the various layers combined into a single layered plate would be integrated ideally into a single composite material using modern materials-by-design methods.

The layered plate not only managed to spread out the shock wave laterally and slow down the shock wave, but it also prevents the projectile from penetrating through the target plate completely. In addition, there is no drastic increase in initial density for the layered plate as compared to the steel plate, which means that there would be no weight penalty for obtaining increased performance.

We believe the concept has now been shown to be successful.

B. RECOMMENDATIONS FOR FUTURE WORKS

1. Exploring Existing Materials

Actual real material definition will take place in future research efforts. There is also a need to investigate composite materials where one layer will have

more than one specific desirable property. If the material is not available, there may be a need to use state-of-the-art material-by-design techniques to ensure that the material has the desired properties. In particular, the wave- spreading layer can be replaced by an orthotropic material in future simulations, and desirable properties for a real material defined.

2. Simulation Setup

Successful and accurate simulation requires careful consideration and continued refinement of material models. Future simulations would include the replication of simulations that more accurately represent experimental work. It is also proposed that the projectile be simulated in more realistic shape for future simulations so as to test penetration effects. In addition, more work is needed to be able to use other materials in AUTODYN^{TM}. In particular, the orthotropic material treatment needs to be tested and made to work, and a model for a polymeric foam implemented.

3. Experimental Testing

Finally, the optimized concepts from finding the real materials need to be fine-tuned before building the prototype for experimental testing. In that way, calculated results can be directly compared with experimental results. This can guide future simulations to increase calculational fidelity. Experimental tests can be simply done at a firing facility. Penetration is relatively simple to diagnose; either the bullet is stopped or it is not.

APPENDIX A. NOTATION

A. GLOSSARY OF TERMS AND NOTATION

This appendix is a glossary of terms and notation used throughout this thesis.

c	Bulk Sound Speed
s	Constant giving Slope of Shock Velocity / Particle Velocity Relationship
G	Shear Modulus
Y	Yield Stress
σ_{spall}	Spalling Failure
ρ_{porous}	Porous Density
C_{porous}	Porous Sound Speed
P_E	Initial Compaction Pressure
P_s	Solid Compaction Pressure
C_{11}	Stiffness Matrix Coefficients
C_{22}	Stiffness Matrix Coefficients
C_{33}	Stiffness Matrix Coefficients
C_{12}	Stiffness Matrix Coefficients
C_{23}	Stiffness Matrix Coefficients
C_{31}	Stiffness Matrix Coefficients
G_{12}	Shear Modulus 12
G_{23}	Shear Modulus 23
G_{31}	Shear Modulus 31

σ_{11}	Tensile Failure Stress 11
σ_{22}	Tensile Failure Stress 22
σ_{33}	Tensile Failure Stress 33
σ_{12}	Maximum Shear Stress 12
σ_{23}	Maximum Shear Stress 23
σ_{31}	Maximum Shear Stress 31
ε_{11}	Tensile Failure Strain 11
ε_{22}	Tensile Failure Strain 22
ε_{33}	Tensile Failure Strain 33
ε_{12}	Maximum Shear Strain 12
ε_{23}	Maximum Shear Strain 23
ε_{31}	Maximum Shear Strain 31
K	Bulk Modulus
D1	Damage Constant 1
D2	Damage Constant 2
D3	Damage Constant 3
D4	Damage Constant 4
D5	Damage Constant 5

LIST OF REFERENCES

[1] Y.M. Gupta and J.L. Ding, “Impact load spreading in layered materials and structures: concept and quantitative measure,” Int. J. of Impact Eng. 27, 2002, pp. 277-291.

[2] Y.M. Gupta, J.L. Ding, and J. R. Robbins, “Load spreading and penetration resistance of layered structures – a numerical study,” Int. J. of Impact Eng. 30, 2004, pp. 593-615.

[3] Army Ammunition Data Sheets for Small Caliber Ammunition, Headquarters, Department of the Army, Technical Manual 43-0001-27, 1994.

[4] Century Dynamics, Users Manual Revision 4.3, Century Dynamics, 2003.

[5] Century Dynamics, Theory Manual Revision 4.3, Century Dynamics, 2003.

[6] Physics of high velocity impact, weapon lethality, and survivability lecture notes, Naval Postgraduate School, 2008.

[7] W. Herrmann, “Constitutive equation for the dynamic compression of ductile porous materials,” J. Appl. Phys., vol. 40, pp. 2490-2499, 1969.

[8] B.M. Butcher, M.M. Carroll, and A.C. Holt, “Shock-wave compaction of porous aluminum,” J. Appl. Phys., vol. 45, No. 9, pp. 3864-3875, 1974.

THIS PAGE INTENTIONALLY LEFT BLANK

INITIAL DISTRIBUTION LIST

1. Dudley Knox Library
   Naval Postgraduate School
   Monterey, California

2. Dr. Robert S. Hixson
   Naval Postgraduate School
   Monterey, California

3. Dr. Jose O. Sinibaldi
   Naval Postgraduate School
   Monterey, California

4. Dr. James H. Luscombe
   Naval Postgraduate School
   Monterey, California

5. Dr. Ronald E. Brown
   Naval Postgraduate School
   Monterey, California

6. Professor Yeo Tat Soon, Director
   Temasek Defence Systems Institute
   National University of Singapore
   Singapore

7. Tan Lai Poh (Ms), Assistant Manager
   Temasek Defence Systems Institute
   National University of Singapore
   Singapore